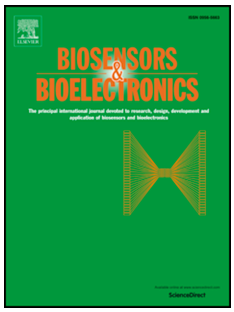

Antibody-Gold Nanoparticle Bioconjugates for Biosensors: Synthesis, Characterization and Selected Applications

Lu Zhang, Yacine Mazouzi, Michèle Salmain, Bo Liedberg, Souhir Boujday

PII: S0956-5663(20)30364-X

DOI: https://doi.org/10.1016/j.bios.2020.112370

Reference: BIOS 112370

To appear in: *Biosensors and Bioelectronics*

Received Date: 30 April 2020

Revised Date: 4 June 2020

Accepted Date: 5 June 2020

Please cite this article as: Zhang, L., Mazouzi, Y., Salmain, Michè., Liedberg, B., Boujday, S., Antibody-Gold Nanoparticle Bioconjugates for Biosensors: Synthesis, Characterization and Selected Applications, *Biosensors and Bioelectronics* (2020), doi: https://doi.org/10.1016/j.bios.2020.112370.

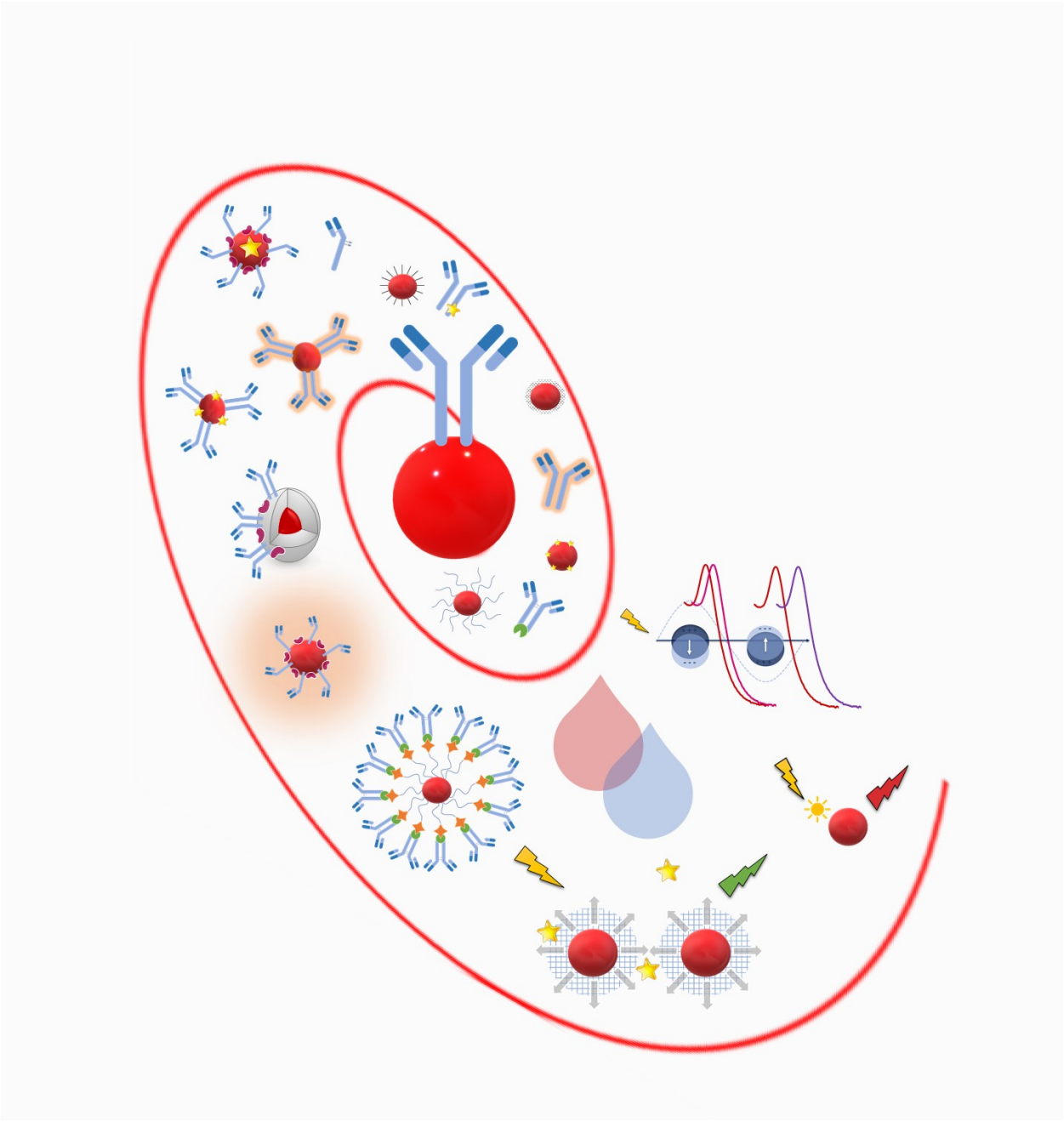

Antibody-Gold Nanoparticle Bioconjugates for Biosensors: Synthesis, Characterization and Selected Applications

Lu Zhang[1,2,3], Yacine Mazouzi[1], Michèle Salmain[2], Bo Liedberg[3], and Souhir Boujday[1]*

[1] Sorbonne Université, CNRS, Laboratoire de Réactivité de Surface (LRS), 4 place Jussieu, F-75005 Paris, France.

[2] Sorbonne Université, CNRS, Institut Parisien de Chimie Moléculaire (IPCM), 4 place Jussieu F-75005 Paris, France.

[3] Centre for Biomimetic Sensor Science, School of Materials Science and Engineering, Nanyang Technological University, 637553 Singapore.

Laboratoire de Réactivité de Surface, UMR CNRS 7197, *Sorbonne Université,* case 178, 4 Place Jussieu, 75252 Paris cedex 05, France

Tel: +33144276001, Fax: +33144276033, souhir.boujday@sorbonne-universite.fr

Tables: 3

Figures: 21

Keywords

Gold nanoparticles; Immunoglobulin G; Localized Surface Plasmon Resonance (LSPR); ligand quantification; Surface Enhanced Raman Scattering (SERS); Fluorescence

Abstract

Antibody-Gold nanoparticle (Ab-AuNP) bioconjugates are widely used in the field of biosensing. This prompted researchers to set up various strategies to conjugate antibodies to gold nanoparticles. Optimal conjugation is of critical importance, as the Ab-AuNP bioconjugates should be stable while maintaining the ability of the antibody to recognize and bind its corresponding antigen. All the same, a high coverage of antibodies on AuNPs is a key-step to build up a sensitive biosensor, but an ideal coverage requires to be perfectly balanced with the orientation and accessibility of the conjugated antibodies. In this review, we intend to provide the reader with the key elements allowing for mastering the conjugation of Ab to AuNP and rationalizing, at the molecular level, the mechanisms involved together with the expected antibody coverages and orientations. We will focus on IgG-type antibodies conjugated to spherical AuNPs as these bioconjugates are the most commonly used ones for biosensors. First, we report an exhaustive survey of the methods of conjugation, *via* strategies of physisorption and chemisorption. Then we provide a critical restitution of the relevant strategies allowing the quantification of antibodies coverage on gold nanoparticles either through direct analysis of the bioconjugates or indirect analysis of the supernatant. In the last part, we review and discuss selected applications of these Ab-AuNP bioconjugates in optical biosensing.

1. Introduction

Plasmonic nanoparticles (NPs) made of coinage metals have drawn a large interest as transducers in the development of optical biosensors owing firstly to their high surface area-to-volume ratio. Secondly, their popularity mostly stems from the so-called localized surface plasmon resonance (LSPR) phenomenon that occurs when an incident light wave is trapped within conductive nanoparticles smaller than the wavelength of the incident light. The conduction band electrons in the NPs collectively oscillate at a resonance frequency induced by the incident wave (Faraday, 1857; Mie, 1908). As a result, plasmonic NPs absorb and/or scatter light very intensely at certain wavelengths, which translates into characteristic bands in their extinction spectrum.

The LSPR band position depends on the composition of the NPs (Ag, Au, Cu, alloys), their shape, their size and the inter-particles distance (Kelly et al., 2003; Loiseau et al., 2019a). Among all the plasmonic NPs, gold nanoparticles (AuNPs) have been widely used in optical biosensing (Li et al., 2010), mostly because of their ease of synthesis and functionalization, high stability, biocompatibility and inertness. Historically, the very first example of use of Ab-AuNP bioconjugates in a biological context was for immunogold labeling of biological samples for transmission electron microscopy imaging (De Mey et al., 1981; Ghosh and Ghosh, 1984; Horisberger et al., 1975;

Horisberger and Rosset, 1977; Tokuyasu, 1983). Furthermore, as briefly mentioned above, AuNPs also display remarkable optical properties. For example, 10 nm-diameter spherical AuNPs display an absorption band in the visible range (λ_{max} = 520 nm) with extremely high extinction coefficient (Jain et al., 2006). This unique property prompted the development of lateral flow assay (LFA) devices using AuNPs as reporter. These single-use devices use immunochromatographic test strips, providing simple, rapid, low cost, and user-friendly detection of various analytes (Hsu, 1984; Moeremans et al., 1984). Another extremely useful property of plasmonic NPs is the sensitivity of the LSPR band to minor changes of the dielectric constant / refractive index (RI) of the local environment. This property enables detection of binding events through standard absorption spectroscopy measurements or even by visual detection (Aldewachi et al., 2018; Loiseau et al., 2019b; Saha et al., 2012; Sepulveda et al., 2009; Tang and Li, 2017). In 1988, Englebienne was the first to exploit the LSPR peak shift induced by the binding of an antigen to Ab-AuNP bioconjugates to determine their dissociation constant (Englebienne, 1998). Furthermore, AuNPs are also able to enhance other optical signals like fluorescence and light scattering (Cho et al., 2018; Hong and Kang, 2006; Liu et al., 2008).

The successful application of antibody-AuNP (Ab-AuNP) bioconjugates in biosensing requires the development of rugged and reliable methods which will ensure that the resulting biosensor is selective, sensitive and reproducible. An efficient bioconjugation method should maintain the colloidal stability of the NPs without impairing the ability of the Ab-AuNP bioconjugates to recognize their antigen. Antibody conjugation can be achieved by physical adsorption, as initially performed by Englebienne (Englebienne, 1998) or *via* chemisorption. The chemisorption of antibodies on planar gold surfaces was widely investigated (Boujday et al., 2008; Thébault et al., 2010). The optimization of antibodies attachment in terms of specificity and accessibility is made possible thanks to classical surface analytical techniques like infrared spectroscopy, quartz crystal microbalance with dissipation measurement (QCM-D), ellipsometry or surface plasmon resonance (SPR) (Boujday et al., 2009). However, let us keep in mind that the optimal adsorption method of antibody on AuNPs may vary from that on planar gold substrates because the stability of colloidal AuNPs is an additional parameter to be considered. Another important parameter to take into account when building up an LSPR biosensor is the distance dependence of the sensitivity to the RI change, requiring the binding event to occur at close proximity of the nanoparticle, unlike planar surfaces where the use of a binding protein like Protein A is often preferred (Boujday et al., 2008).

In what follows, we will review the strategies allowing for engineering Ab-AuNP bioconjugates with a focus on IgG-type antibodies and spherical AuNPs. First, we will address the existing methodologies for antibodies attachment to AuNP. Then we will investigate the challenging question of the quantification of antibodies on AuNPs surface. Through this review, we intend to provide the reader with key elements allowing for mastering the conjugation of Ab to AuNP and rationalizing, at the molecular

level, the mechanisms involved together with the expected antibody coverages, often over-estimated. Ab-AuNP bioconjugates have indeed become a cornerstone for a significant number of biomedical applications beyond biosensors, like therapeutic and theranostic covered by the following literature reviews (Biju, 2014; Carter et al., 2016). In the last part of this review we will recap the potential of these bioconjugates for optical biosensing through a selection of relevant applications.

2. Bioconjugation methods

In this section, we review the different strategies that have been applied for the conjugation of antibodies to gold nanoparticles (AuNPs). These strategies are based on physisorption or chemisorption *via* modification of antibody and/or of AuNPs (Fig. 1).

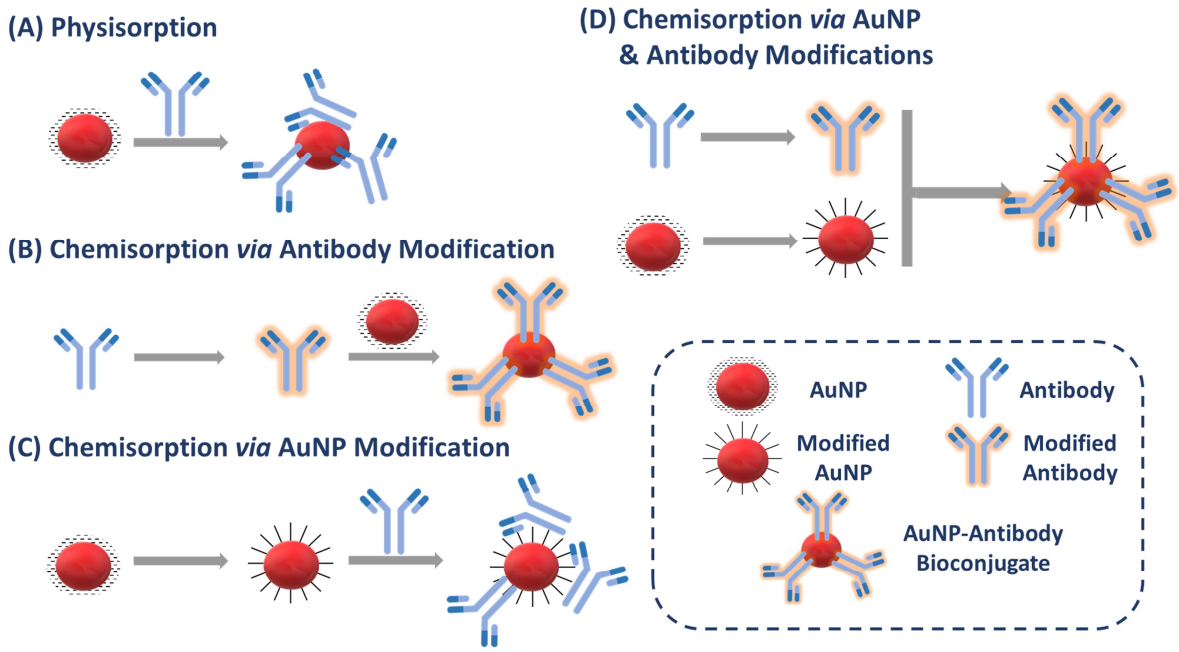

Fig. 1 : Conjugation of antibodies to gold nanoparticles *via* (A) physisorption or chemisorption *via* (B) modification of antibody, (C) modification of gold nanoparticle, (D) modification of antibody and gold nanoparticle.

2.1. Physisorption

Physisorption is generally established through electrostatic, hydrogen bonding, hydrophobic, and van der Waals attractive forces between AuNP and antibody. It is the simplest and most straightforward conjugation method. It requires minimal expertise in surface chemistry. Its easiness is based on the fact that it is not necessary to chemically modify the antibody nor the AuNP.

During the preparation of antibody-AuNP (Ab-AuNP) bioconjugates by physisorption, several parameters should be considered: (a) the isoelectric point (pI) of the antibody, (b) the pH, and (c) the added quantity of antibody (Geoghegan, 1988). It is generally agreed that maximal adsorption of proteins occurs when the pH is close to or slightly above their pI (Bagchi and Birnbaum, 1981; Demanèche et al., 2009; Geoghegan and Ackerman, 1977; Hook et al., 1998; Peng et al., 2004). For many proteins, especially antiserum-derived immunoglobulins, the average pI spans over a broad range of pH values (Geoghegan, 1988). The optimal coupling pH value for a given antibody should be determined through measurement of its relative pI range. In practice, conjugation is tested at different pH to find the optimal value. However, many antibodies are best adsorbed at a pH 8-9. Next, the added quantity of antibody for adsorption is determined by the flocculation test. This test is used to determine the minimum amount of antibody required to maintain AuNP stability against salt-induced aggregation, *e.g.* 10% NaCl. Aggregation may be monitored by the color change of the colloidal solution or by measuring the absorbance of the solution at its λ_{max} (Horisberger et al., 1975). In practice, the final added amount of antibody is the minimum amount plus 10% - 20% (De Mey et al., 1981; Horisberger and Rosset, 1977) to produce the Ab-AuNP bioconjugates. Finally, many protocols include a subsequent step to stabilize the conjugate suspension by addition of polyethylene glycol (PEG, 1%) (El-Sayed et al., 2005; Horisberger et al., 1975; Horisberger and Rosset, 1977) or bovine serum albumin (BSA, 0.25%) (De Mey et al., 1981; Hermanson, 2008a). These blocking agents also mask any remaining free sites on AuNP, thus preventing further nonspecific binding (Lai et al., 2015). Most protocols of antibody physisorption to AuNP follow the steps mentioned above (Lou et al., 2012; Rayavarapu et al., 2007; Safenkova et al., 2010; Zhang et al., 2019a).

Tokuyasu reported that addition of a large excess of protein to AuNP suspension yields conjugates with high specific activity (Tokuyasu, 1983). Nevertheless, there was evidence that overloading may cause progressive loss of loosely bound protein (Horisberger and Clerc, 1985). Byzova et al. found that antibody concentration used for conjugation can be reduced below the stabilizing concentration without losing antigen-capturing activity of the conjugates (Byzova et al., 2017). Hence, the optimal antibody concentration should be chosen for each individual case considering the colloidal stability and retention of antibody activity. Besides the factor of antibody concentration, Geng et al. showed that additional purification of synthesized AuNPs prior to conjugation to polyclonal antibody at acidic pH improved the reproducibility of conjugate preparation and this conjugate displayed excellent analytical performances (Geng et al., 2016).

Despite its easiness, physisorption of antibody to AuNP displays two main drawbacks: (1) the antibody is randomly immobilized on AuNP. This may cause partial loss of antigen binding capacity due to direct interaction between AuNP and the antigen binding sites or steric hindrance with 'head-on' and 'side-on' spatial orientations, as shown in Fig. 2. and (2) the attachment is weak. Nevertheless, by carefully controlling

the pH of the antibody solution between 7.5 and 8.5 and thus the antibody surface charge, it was possible to finely tune the orientation of the antibody molecules at the surface of citrate-coated AuNP, and in turn modulate the immunoactivity toward its antigen (Ruiz et al., 2019). Under binding equilibrium, AuNP-bound and free antibody co-exist in the conjugate sample and multilayer adsorption of antibodies may occur. The loosely bound layers, except from first and second ones, may desorb, thus making the conjugates less stable over time.

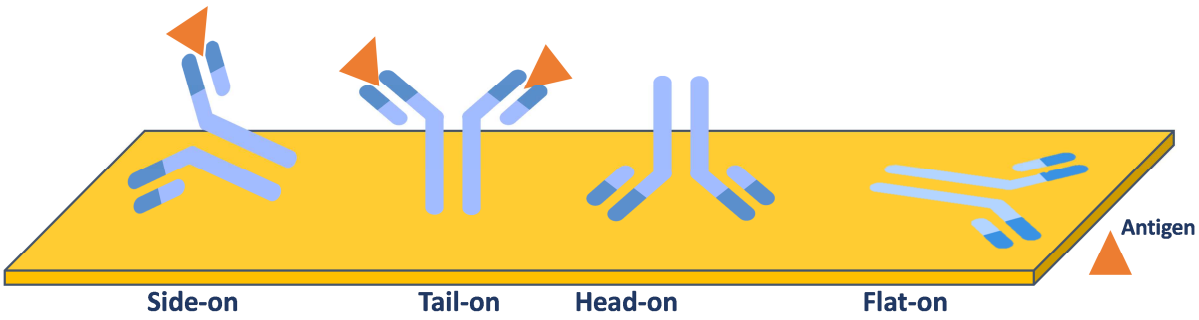

Fig. 2 : Possible spatial orientations of antibody on surface.

2.2. Chemisorption

Chemisorption of antibody is more chemically demanding than physisorption, but the former method generally provides higher stability of immobilized antibodies, improved epitope presentation and thereby better reproducibility of the antibody-antigen binding events. It requires several steps including chemical modification of antibody or/and AuNP prior to conjugation depending on the selected coupling chemistry.

2.2.1. Chemical modification of antibody

The sulfhydryl group is very attractive for conjugation of antibody to AuNP since it forms a strong Au-S bond. However, there are no free sulfhydryl groups in IgG-type antibodies (Hermanson, 2008b). Thus, sulfhydryl groups need to be created by reaction of appropriate thiolation reagents or generated by reduction of endogenous disulfide bridges of cystine residues. In what follows, we will discuss modification of functional groups on antibodies used for covalent binding, including common groups such as amine and carbohydrate moieties, disulfides, and also special sites like the nucleotide binding site (NBS) (Fig. 3). Depending on the method, orientation of antibody molecules with respect to AuNP will be either random or controlled.

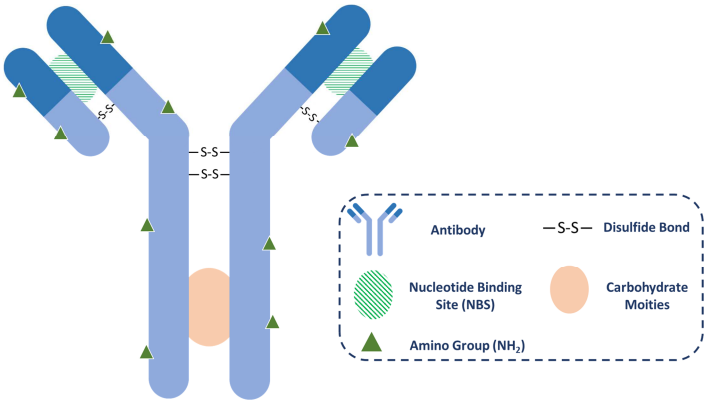

Fig. 3 : Important functional groups on immunoglobulin G (IgG).

2.2.1.1. Generation of sulfhydryl groups from amino groups

Primary amino groups are abundant in antibodies. They are randomly distributed all over the IgG molecules and are mostly located at the surface owing to their polarity and charge (positive at physiological pH). They are carried by the side chain of the ca. 70 lysines and the N-terminus of the light and heavy chains of IgG (Nisnevitch and Firer, 2001). In addition, amines are very reactive towards many reagents without any previous activation owing to their nucleophilic character.

For example, Traut's reagent (2-iminothiolane) undergoes ring-opening reaction with a primary amine to generate a sulfhydryl group (Fig. 4A). This process is very efficient and proceeds rapidly at slightly basic pH (Hermanson, 2008b, c). It has been successfully applied by us and other groups to immobilize IgG on AuNP (Ben Haddada et al., 2017; Wang et al., 2017).

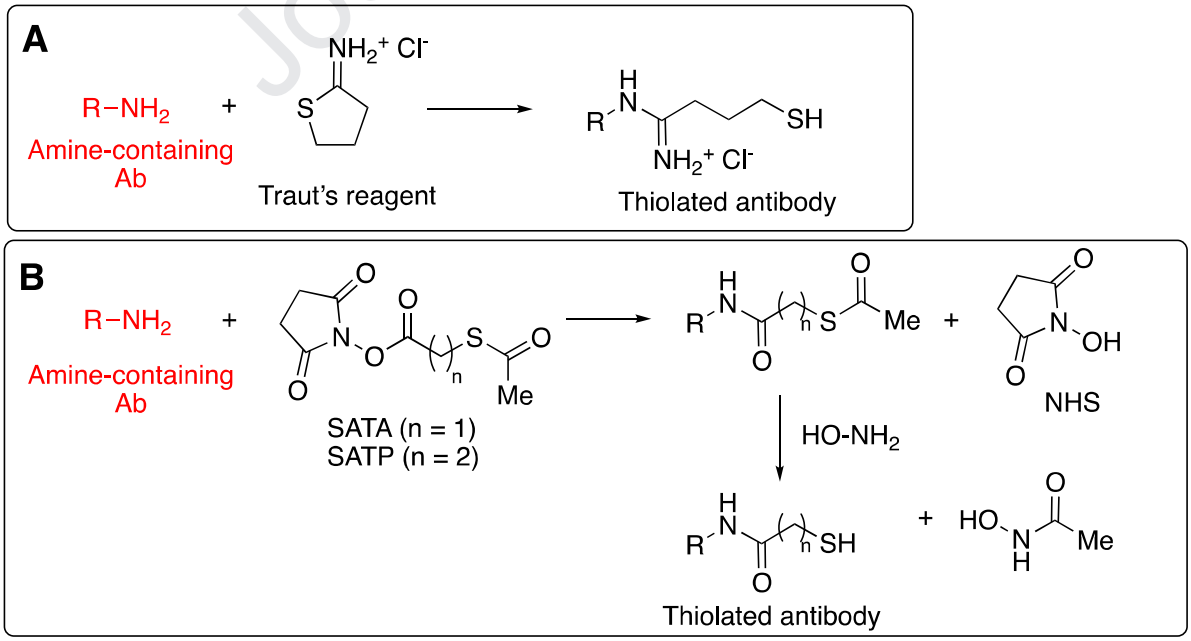

Fig. 4 : Reaction of thiolation reagents with primary amines: A. Traut's reagent (2-

iminothiolane) and B. N-succinimidyl S-acetylthioacetate (SATA) or N-succinimidyl S-acetylthiopropionate (SATP).

Since Bragg and Hou introduced N-hydroxysuccinimide (NHS) esters to activate carboxylic acids in 1980 (Bragg and Hou, 1980), they became the major amine-coupling reagents in bioconjugate chemistry as a result of their excellent reactivity toward primary amines at physiological pH. For instance, Duncan et al. (Duncan et al., 1983) have synthesized N-succinimidyl S-acetylthioacetate (SATA). SATA reacts with proteins' amino groups forming stable amide linkages and protected sulfhydryl groups in the form of thioesters (Fig. 4B). Such a protecting group can be released with hydroxylamine to form free –SH just before conjugation to AuNP (Hermanson, 2008d). Similarly, N-succinimidyl S-acetylthiopropionate (SATP) is also used to introduce sulfhydryl groups into proteins (Fig. 4B). Modification of proteins by of SATA or SATP is straightforward and as this is done under mild conditions, it leads to little loss of the protein function or activity. Both these reagents have been applied by researchers for antibody modification prior to conjugation to AuNP (Das et al., 2011; Kao et al., 2013; Vdovenko et al., 2016).

In addition, disulfide bond-containing NHS esters are very attractive for antibody modification as disulfides themselves self-assemble on AuNP by formation of Au-S bonds. For example, the molecules gathered in Fig. 5, 3,3'-dithiobis(succinimidyl propionate) (DSP), 3,3'-dithiobis(sulfosuccinimidyl propionate) (DTSSP) (Filbrun et al., 2017), N-succinimidyl 3-(2-pyridyldithio)propionate (SPDP) (Van Der Heide and Russell, 2016), and N-succinimidyl 6-(3(2-pyridyldithio)propionamido)hexanoate (LC-SPDP) (Liao and Hafner, 2005) have been used to modify amino groups of antibody prior to chemisorption to AuNP. A reagent including a PEG linker, like OPSS-PEG-NHS commercialized by Creative PEGWorks (Fig. 5) was also applied for the same purpose (Day et al., 2010). The long PEG linker enables to increase the distance between the antibody and the AuNP, decreasing the risk of steric hindrance. At the same time, PEG also helps to prevent nonspecific protein binding to AuNP.

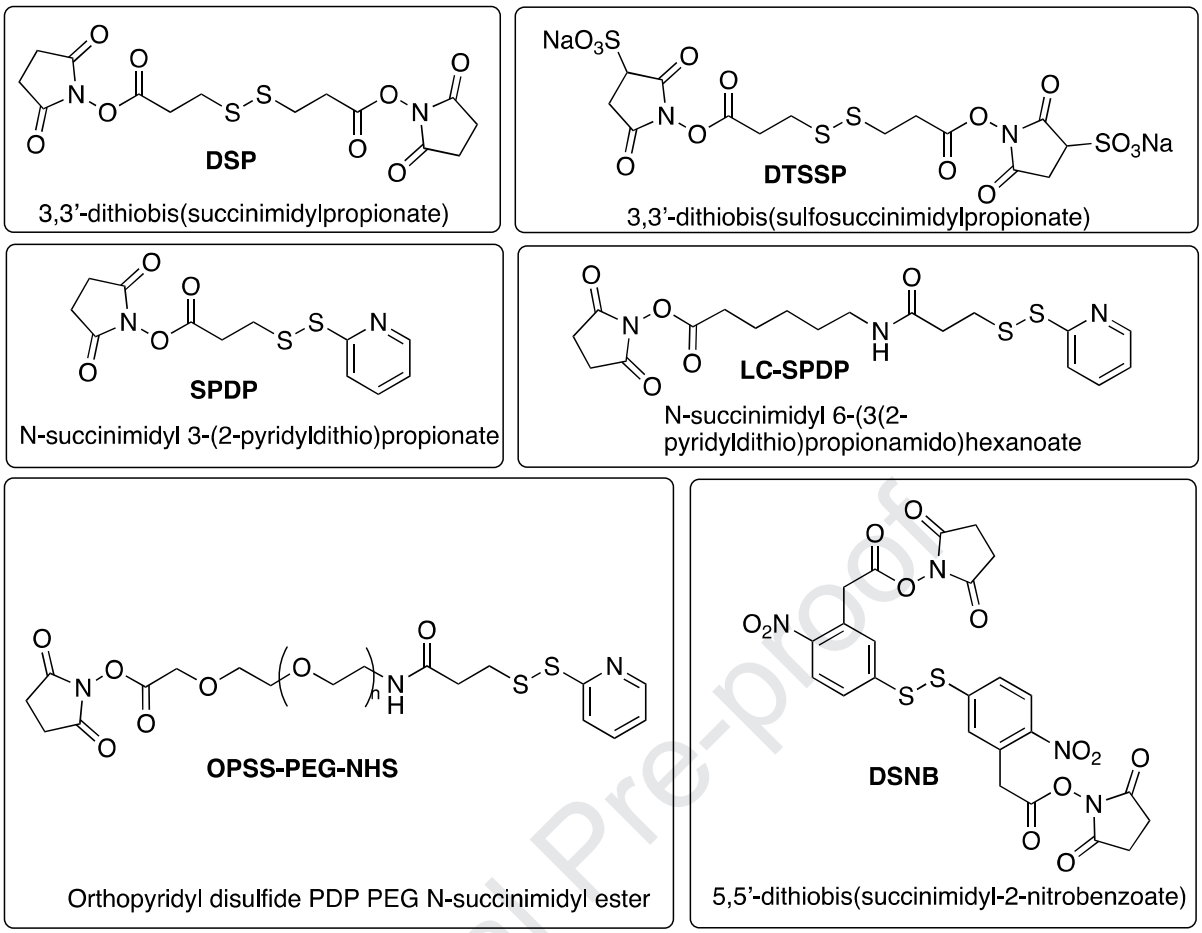

Fig. 5 : A selection of disulfide-bond containing NHS ester molecules used for Ab attachment to AuNPs.

However, amine reactive coupling chemistry *via* NHS esters presents a major drawback owing to the rapid hydrolysis of NHS esters whose rate is comparable to the acylation rate (Lim et al., 2014). Thus, a large excess of antibody is required to favor the acylation reaction. All these strategies result in non-selective chemical modification of primary amines on the antibody surface and to randomly oriented antibody molecules on AuNP.

2.2.1.2. Generation of sulfhydryl groups from carbohydrate groups

The fragment crystallizable region (Fc region) of polyclonal IgG produced by the major mammalian species (rabbit, goat and so on) contains carbohydrate chains (Fig. 3). Covalent binding through these sugar moieties offers controlled orientation of the antibody molecules with respect to the AuNP surface and is thereby less likely to alter the capacity of the Ab-AuNP bioconjugates to bind their target antigen owing to the long distance between the paratopes and the conjugation site. This strategy requires a first step in which the carbohydrates are mildly oxidized by sodium periodate ($NaIO_4$) to create reactive aldehydes. Then aldehyde-activated sugars react with 2-acetamido-4-mercaptobutyric acid hydrazide (AMBH), forming acyl hydrazone linkages and sulfhydryl groups. The formed Schiff base may be further reduced with sodium cyanoborohydride to afford a stable hydrazide bond (Fig. 6A) (Hermanson, 2008b). Heterobifunctional PEG linkers, like monothiol-PEG-hydrazide or dithiol-PEG- hydrazide

(Fig. 6B and C) have also been used by different research groups for the same purpose (Ciaurriz et al., 2017; García-Fernández et al., 2017; Joshi et al., 2013; Kumar et al., 2008; Raoof et al., 2012).

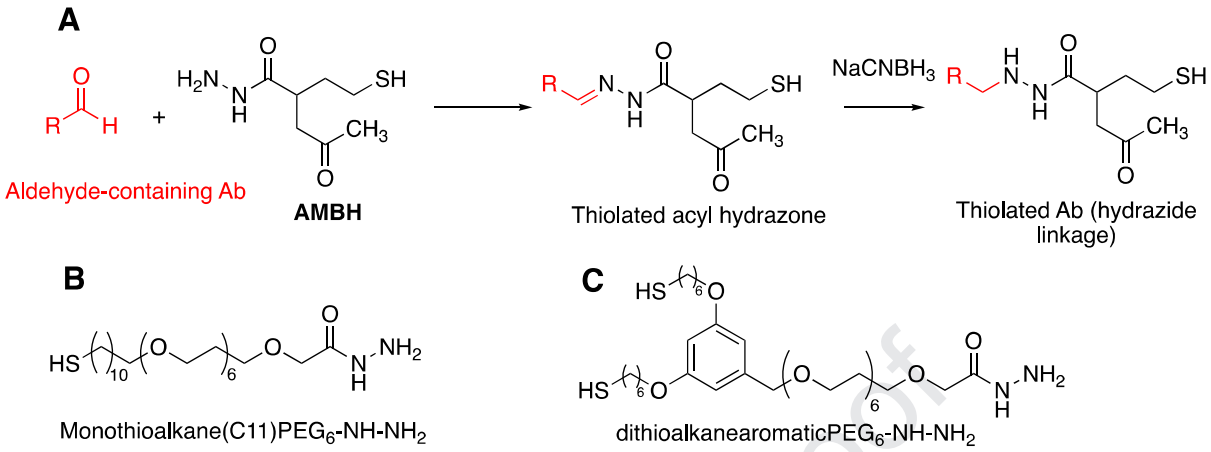

Fig. 6 : A: Reductive amination reaction between hydrazide and aldehyde, B and C: Commercial thiol-PEG- hydrazide linkers.

A major limitation of this approach is that the antibody must be glycosylated. Polyclonal antibodies (from antisera) usually are, but other antibody preparations such as recombinant antibodies fermented in bacteria, or some monoclonal antibodies that did not undergo post-translational glycosylation may not have carbohydrates. Note that, if the acyl hydrazone reduction step is omitted, the bond between the antibody and the AuNP can be easily cleaved by decreasing the pH below 6 leading to antibody desorption (Raoof et al., 2012).

2.2.1.3. Generation of sulfhydryl groups by disulfide reduction

Antibody can be directly immobilized on gold surfaces by using a UV light-induced approach, known as photochemical immobilization technique (PIT) as shown in Fig. 7 (Neves-Petersen, 2006). Briefly, tryptophan residues absorb UV light and relax by transferring the absorbed energy to their neighbors. If a cystine (formed by 2 cysteines bound together by a disulfide bridge) is close enough to the tryptophan, the photon energy is virtually absorbed by cystine, leading to the cleavage of the disulfide bridge. The resulting free thiol groups can anchor efficiently to gold substrates (Della Ventura et al., 2011). This is a mild method preserving the structural and functional properties of antibody. An optical immunosensor based on Ab-AuNP conjugate prepared by the PIT method showed a good sensitivity and an extended linear range for the assay of human IgG (Iarossi et al., 2018).

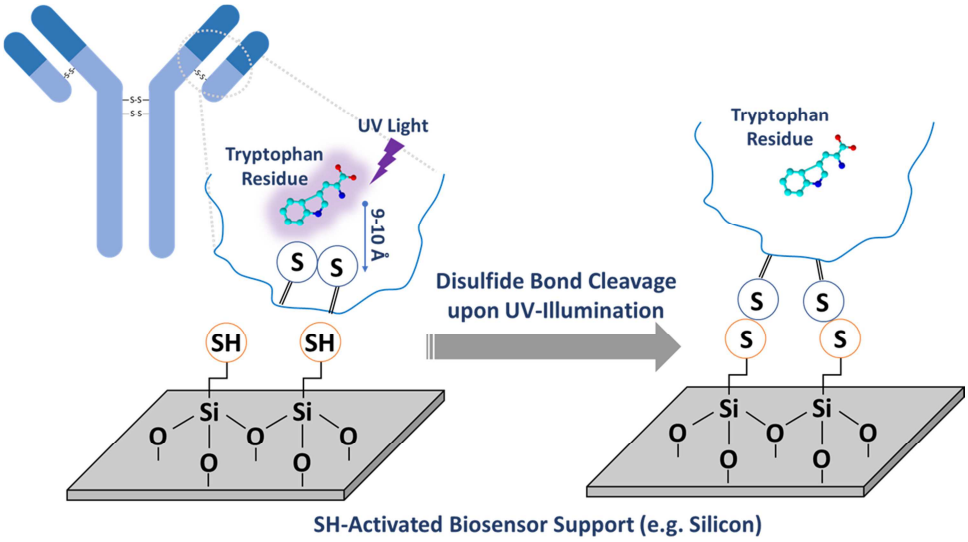

Fig. 7 : Illustration of the photochemical immobilization technique (PIT). Tryptophan residues absorb UV light and release the absorbed energy to a nearby cystine residue (S-S) that dissociates to form cysteine residues (SH) for reaction with surface SH groups. Picture is adapted from ref. (Neves-Petersen, 2006).

As mentioned above, all the cysteine residues of mammalian antibodies are engaged in disulfide bridges, and they are important to the antibody function as they contribute to the tertiary structure of each antibody subunit (intrachain S-S bridges). They also covalently connect the heavy to the light chains and the two heavy chains at the hinge region (interchain S-S bridges) (Fig. 8A). As only free sulfhydryl groups of antibody can be conjugated directly to AuNP, the native disulfide bonds must be selectively cleaved by reducing agents while preserving the antigen-binding capacity. The reduction of antibody disulfide bonds is affected by several factors, for example, antibody host, pH, reductant and reductant concentration. By careful manipulation of these factors, high yield of half-antibody fragments can be obtained by selective cleavage of the S-S bridges of the hinge region (Makaraviciute et al., 2016).

For instance, in the presence of a moderate concentration of dithiothreitol (DTT, Fig. 9A) and absence of denaturant (such as urea, guanidine or SDS), cleavage of disulfide bridges of antibodies mainly occurs at the hinge region (rabbit and goat IgGs have two disulfide bridges in this region) (Bewley and Li, 1969; Vikholm-Lundin and Albers, 2006; Wang et al., 2017). Other reducing reagents, such as 2-mercaptoethanolamine (2-MEA, Fig. 9B) (Karyakin et al., 2000; Makaraviciute et al., 2014; Wang et al., 2005) and tris(2-carboxyethyl)phosphine (TCEP, Fig. 9C) (Mustafaoglu et al., 2017; Sharma and Mutharasan, 2013; Wang et al., 2013) have also been used for antibody reduction. Both 2-MEA and DTT contain thiol groups that may compete with the reduced antibodies at the adsorption step to AuNP. Therefore, the reducing agents 2-MEA and DTT need to be removed from the reduced antibody solution prior to the conjugation to AuNP. Such a separation adds one more step to the protocol that may lead to loss of the reduced

antibody and traces of reducing agent may still remain. TCEP (Burns et al., 1991) is a more stable and a stronger reducing agent than 2-MEA and DTT. Since TCEP is sulfur-free reagent, it does not compete with the reduced antibody during its adsorption to AuNP, and therefore, a separation step is not essential. This makes TCEP a more convenient reducing reagent of antibody for chemisorption to AuNP.

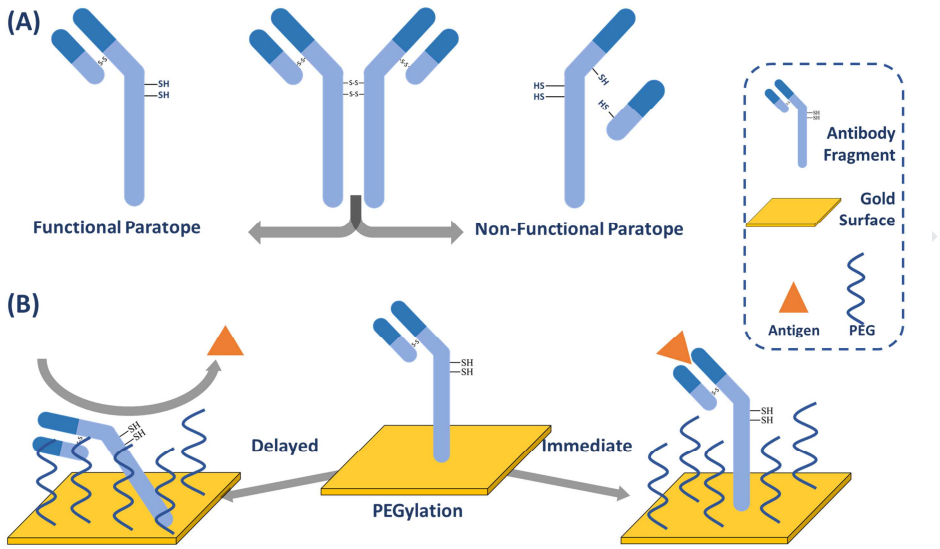

Fig. 8 : A. Generation of free sulfhydryl groups by reduction of antibody leading to antibody fragment with functional or non-functional paratope. B. Illustration of time-dependent inactivation of antibody fragments. Adapted with permission from ref. (Yoshimoto et al., 2010).

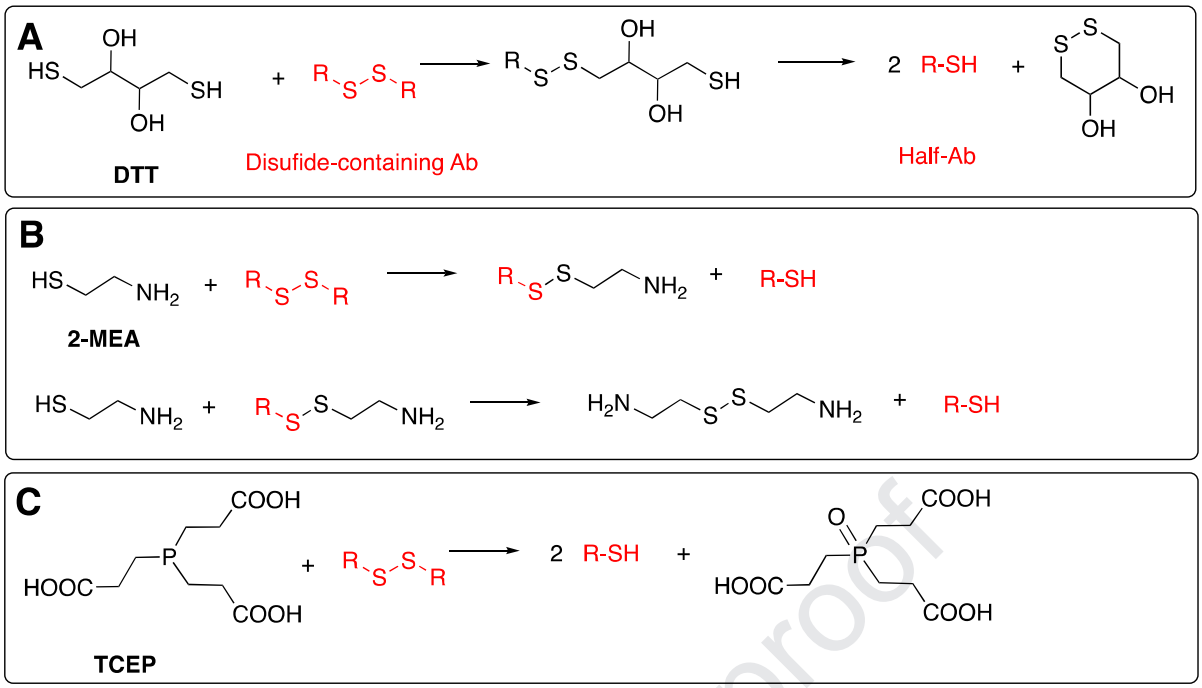

Fig. 9 : Reduction of antibody to half-antibody fragments using A. dithiothreitol (DTT), B. 2-mercaptoethanolamine (2-MEA) and C. tris(2-carboxyethyl)phosphine (TCEP).

Through this strategy, the antigen binding site is directed away from AuNP, and because of the reduced size of half-antibodies, a higher number of antigen binding sites per nm^2 on the AuNP surface can be achieved, thus giving a better antigen binding capacity. Balevicius et al. demonstrated that antibody fragment modified surface interacted with antigens more efficiently in comparison with that modified by intact antibody (Balevicius et al., 2011). However recent studies showed that this strategy induced inactivation of the antigen binding capacity of the antibody fragments due to conformational and/or orientational change of fragments on the gold surface with time. The activity disappeared almost completely 60 min after immobilization. This inactivation can be slowed down if the antibody fragments are immediately co-adsorbed with PEG as shown in Fig. 8B (Yoshimoto et al., 2010).

2.2.1.4. Generation of disulfides *via* the nucleotide-binding site (NBS)

Even across different isotypes, antibodies contain a largely conserved sequence between the heavy and light chains of the antigen-binding fragment F_{ab} region known as nucleotide binding site (NBS, location shown in Fig. 3). By targeting the NBS using a small indole molecule and UV irradiation, oriented immobilization of antibody on planar surface could be achieved. Alves et al. found that this method provided 8-fold better antigen detection sensitivity compared to physical adsorption (Alves et al., 2012). Mustafaoglu et al. applied this method to the conjugation of antibody to AuNP as shown in Fig. 10 (Mustafaoglu et al., 2017). In practice, the indole-containing molecule, tryptamine-PEG_8-lipoamide, was photo-cross-linked to the NBS of antibody upon

exposure to UV light. Then, functionalized antibodies were immobilized on AuNP in an oriented manner *via* S–Au bonds. Mustafaoglu et al. also compared the antigen recognition sensitivity of this system to other conjugation methods, *e.g.* physisorption, EDC-NHS activation, thiol reduction (antibody fragmentation), and concluded that this UV-NBS method gave enhanced antigen detection capability and sensitivity with a high level of selectivity.

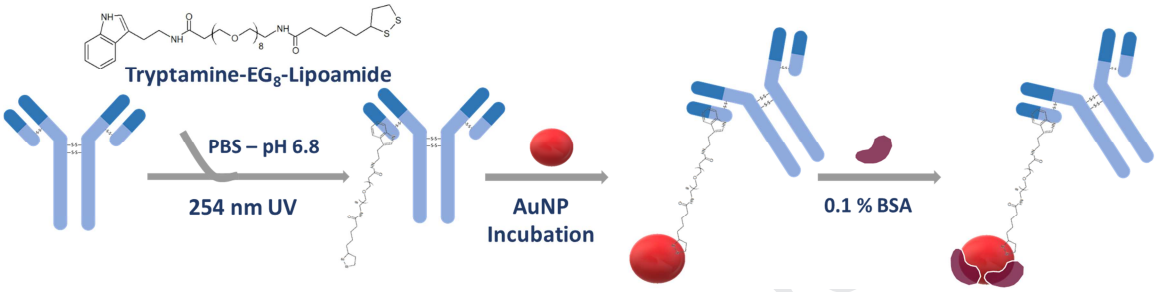

Fig. 10 : Indole derivative used for UV-NBS method and conjugation scheme adapted from ref. (Mustafaoglu et al., 2017).

2.2.2. Modification of AuNP

The surface of AuNP can be decorated with various heterobifunctional ligands containing thiols or disulfides for stable anchoring to the particles and another functional terminal group for conjugation of antibodies (Boujday et al., 2017).

2.2.2.1. Carboxyl or NHS ester groups

Disulfide-containing sulfo-NHS heterobifunctional crosslinker, DTSSP (Fig. 5), was chemisorbed on AuNP followed by conjugation of antibody by reaction of its amino groups (Filbrun and Driskell, 2016; Filbrun et al., 2017). Specific chemical groups could be introduced within the crosslinker for appropriate application. For example, Grubisha et al. synthesized 5,5'-dithiobis(succinimidyl-2-nitrobenzoate) (DSNB, Fig. 5) containing nitroaryl group which gives a strong Raman signal (Grubisha et al., 2003). Alternatively, heterobifunctional PEG linkers (HS-PEG-COOH) were used, for instance, monothiol-PEG-COOH (Ciaurriz et al., 2017; Haller et al., 2015; Hinterwirth et al., 2013; Špringer et al., 2017; Stuchinskaya et al., 2011; Van Der Heide and Russell, 2016) or dithiol-PEG-COOH linker (Eck et al., 2008; Špringer et al., 2017). After self-assembling of linkers on AuNP through Au-S bond, the carboxyl groups were activated into the NHS or sulfoNHS esters using the classical NHS/EDC chemistry, which then reacted with amine groups on the antibody forming stable amide bonds. Coupling of antibody to the NHS-activated AuNP proceeds in a random orientation *via* any free amino groups present on antibody. In this way an antibody can react with more than one AuNP and thus may induce AuNP cross-linking.

2.2.2.2. Fc-binding proteins

Antibody-binding proteins such as protein G/A specifically bind to the Fc region of antibodies. Antibodies immobilized on Fc-binding protein-coated surfaces are therefore properly oriented for optimal epitope presentation and antigen binding. What is more, protein G/A can bind IgG from various sources like rabbit, goat, mouse, human and other mammalian species. As antibody modification is not required for immobilization, bound antibody fully retains its binding ability and is properly oriented on AuNP surfaces. The binding protein A or G must be first immobilized on AuNP either through chemical reaction (Leggett et al., 2007; Van Der Heide and Russell, 2016), or simply physisorbed (James and Driskell, 2013; Tripathi and Driskell, 2018). SPDP was used as reactant to modify Protein A (Leggett et al., 2007; Van Der Heide and Russell, 2016), then the thiolated protein displaced the citrate layer around AuNP. Alternatively, protein G was physically adsorbed on AuNP prior to antibody immobilization (Hinterwirth et al., 2013). In all cases, antibody was subsequently immobilized on AuNP by binding to protein A *via* its Fc region in an oriented configuration. One of the major concerns associated with this method is the additional immobilization process of Fc-binding protein coating on AuNP surface prior to antibody attachment which induces a higher spacing of targets. As LSPR intensity is a local phenomenon, such spacing affects the biosensing readout.

2.2.3. Modification of AuNP and antibody

In some strategies, both AuNP and antibody are modified to generate Ab-AuNP bioconjugates.

2.2.3.1. Michael addition

Thiolated antibody can be covalently attached to maleimide-AuNP by Michael reaction, i.e. addition of sulfhydryl to the double bond of maleimide. Depending on the type of antibody, cleavage of disulfide bonds or addition of sulfhydryl groups is necessary prior to conjugation. For instance, the disulfide bonds at the hinge region of antibody were reduced using the mild reducing agent MEA (Fig. 9B) followed by covalent attachment of antibody fragments to maleimide-AuNP (Rayner and Stephenson, 1997).

2.2.3.2. Reductive amination

The sugar moieties of antibody can be oxidized with $NaIO_4$ creating aldehyde groups. On the other hand, AuNP was decorated with primary amino groups using for instance chemisorption of NH_2-PEG-SH. The stable attachment of antibody to AuNP was realized in the presence of $NaCNBH_3$ (reaction mechanism shown in Fig. 6) (Van Der Heide and Russell, 2016).

2.2.3.3. High affinity association

Biotinylated antibodies can be easily assembled to streptavidin (SAV)-coated AuNP to afford stable conjugates (Inci et al., 2013; Malaspina et al., 2017). Antibody conjugation to AuNP also can be achieved *via* DNA hybridization using specific Watson-Crick base pairing of two complementary nucleic acid sequences. This strategy basically requires a two-step process: conjugation between antibody and single strand DNA sequence and conjugation between AuNP and complementary DNA sequence. Combined with biotin-streptavidin association (Hazarika et al., 2005; Niemeyer and Ceyhan, 2001), directional attachment of antibody on AuNP was achieved. Experimentally, DNA-SAV was prepared from thiolated oligonucleotides and recombinant streptavidin using heterobifunctional cross-linker as shown in Fig. 11A. Then DNA-SAV was assembled to biotinylated antibody through high affinity between biotin and SAV. Complementary capture oligonucleotides were chemisorbed to AuNP through Au-S bond. Eventually, the DNA-SAV conjugated antibody bound to DNA-AuNP *via* Watson-Crick base pairing. Similarly, instead of biotin-SAV, protein G was combined to DNA base pairing for oriented attachment of antibody (Jung et al., 2007) as shown in Fig. 11B. Alternative to DNA hybridization, self-assembly of two monomeric polypeptides also produced permanent and oriented protein attachment to AuNP (Ferrari et al., 2010).

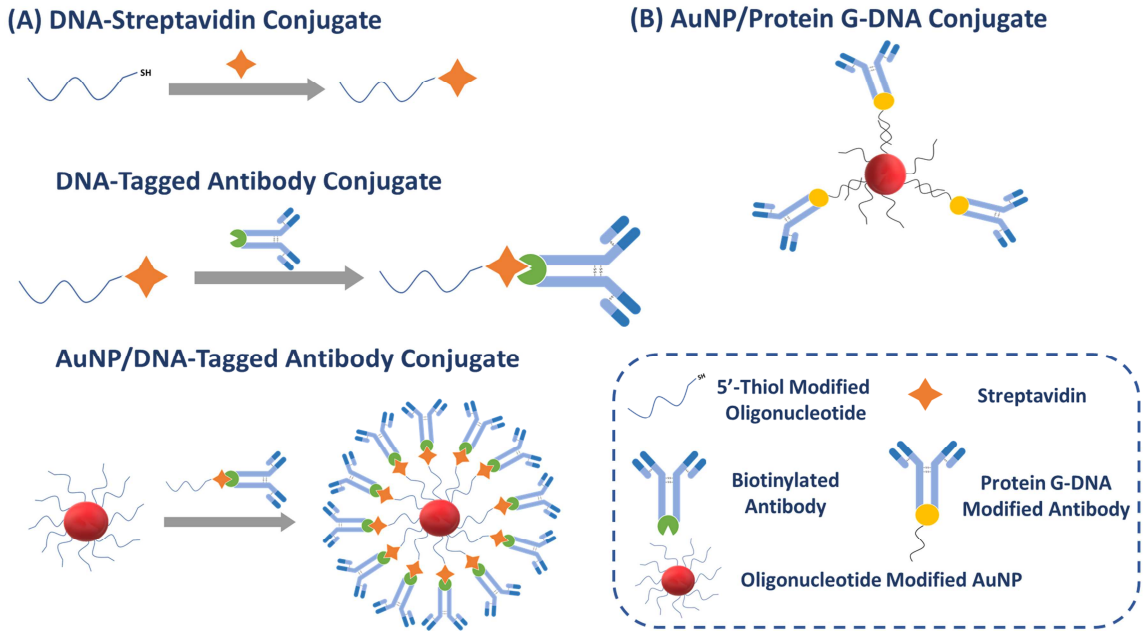

Fig. 11 : DNA sequence combined with (A) biotin-streptavidin (Niemeyer and Ceyhan, 2001) or (B) protein G (Jung et al., 2007).

2.2.3.4. Click chemistry

Antibody was reacted with azido-PEG_8-NHS ester to introduce azido groups on the antibody in a random fashion. On the other hand, a synthetic copolymer coating was grown on AuNP surface, one of the monomers carrying a terminal alkyne functionality (Fig. 12). This thin polymer layer on the surface stabilized the colloidal suspension

(Finetti et al., 2016). Azido-containing antibody was then conjugated to alkyne-carrying AuNP by copper-catalyzed azide-alkyne cycloaddition (Fig. 12).

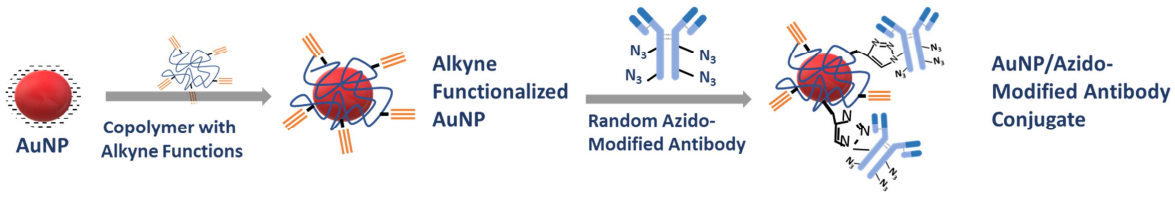

Fig. 12 : Schematic representation of surface modification of AuNP with a synthetic copolymer and subsequent conjugation with azido-modified antibody. Adapted from ref. (Finetti et al., 2016).

2.3. Conclusions of the section

The structural features of antibodies, including their shape, function and chemical stability, make their attachment to AuNP a challenging task. The performance of AuNP-based biosensors is markedly affected by the applied conjugation strategy between antibody and AuNP that in turn controls surface coverage and antibody orientation (García-Fernández et al., 2017; Saha et al., 2014; Tripathi and Driskell, 2018; Welch et al., 2017). In this section, an exhaustive survey of the methods of conjugation of antibody to spherical AuNP, *via* strategies of physisorption and chemisorption, has been presented to provide the reader with key elements allowing for mastering the conjugation of Ab to AuNP. Obviously, the orientation of antibody molecules and how they are linked to the AuNP are important to keep their activity intact for the desired application of the conjugates. This key-factor needs to be balanced with parameters such as relative distance Ab-AuNP or chemical modification of antibodies to adapt to the desired application.

3. Quantification of antibody in Ab-AuNP bioconjugates

It stands to reason that an optimal coverage of antibodies on AuNPs is a key-step to build up an efficient biosensor, and by “optimal” one infers ideal coverage, orientation, and accessibility. Some of the conjugation strategies presented in the previous section allow for the control of antibodies orientation and therefore, of the accessibility of the recognition sites. Most of the conclusions drawn on antibodies orientation once immobilized arise from studies on planar surfaces. For instance, characterization techniques of Ab orientation on planar sensor surface have been reported in ref. (Trilling et al., 2013; Welch et al., 2017). When it comes to nanoparticles, the characterization is far more challenging including for the estimation of antibodies coverage. As a consequence, most quantifications follow an indirect pathway by relying on the supernatant analysis to determine the proteins left in, and thereby, the remaining proteins deduced from the initial amount, assuming that all of the proteins absent from the supernatant are adsorbed on the AuNPs. The direct quantification, i.e. through the

analysis of Ab-AuNP bioconjugates allows for a more accurate estimation of antibodies coverage.

In this section, we will present the different quantitative methods to measure surface coverage of antibody on gold nanoparticles reported to date through direct or indirect strategies. In what follows, we will also analyze and discuss the results of these methods in terms of antibody coverage with respect to the geometrical restrictions. To date, there are two crystal structures published for whole IgG type antibodies, 1IGY (mouse IgG1) and 1IGT (mouse IgG2a) (Harris et al., 1997; Harris et al., 1998). As illustrated in Fig. 13, one can estimate the surface occupied by an antibody depending on its orientation which would lead to the highest coverage for a side-on orientation. We have calculated from this data the expected ratio Ab/AuNP based on the assumption of a spherical shape of AuNP rather than cubo-octahedral for a series of diameters, the most commonly used in the literature. The results gathered in Table 1 will be utilized in what follows to rationalize the data determined from both indirect and direct quantification.

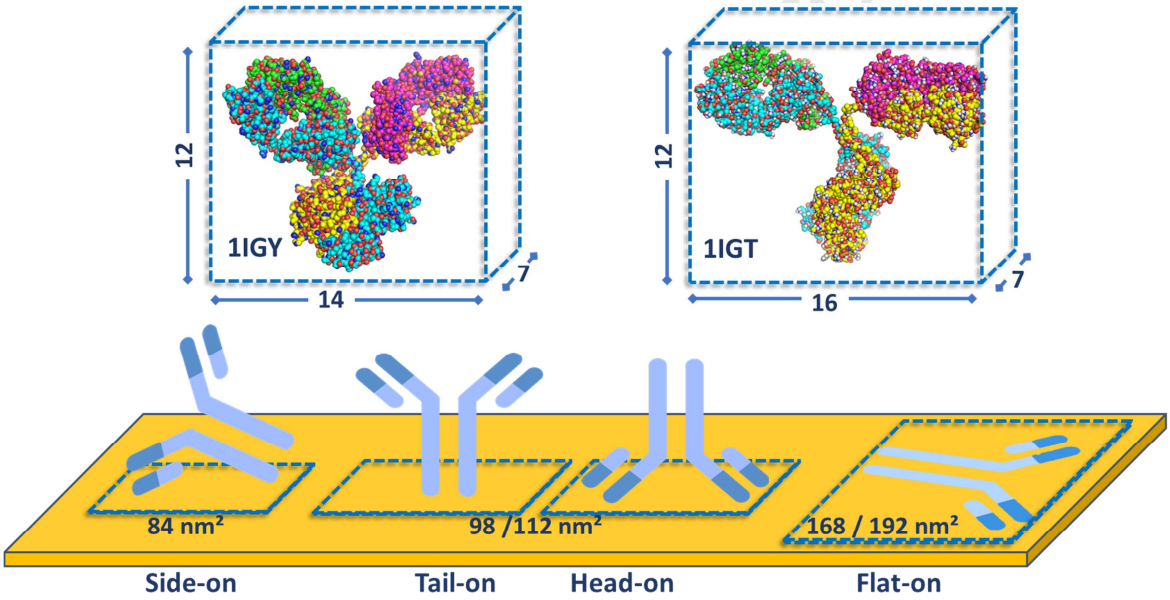

Fig. 13 : X-ray structures of mouse IgG1 (1IGY) and mouse IgG2a (1IGT) from references (Harris et al., 1997; Harris et al., 1998), projected within a sized cuboid and the resulting footprint area occupied upon adsorption, depending on the Ab orientation.

Table 1: Maximal Ab/AuNP ratios calculated from geometrical restriction depicted in Fig. 13

AuNP Diameter	Side-on	Tail-on/Head-on	Flat-on	Size to scale
10 nm	3.7	3.2	1.9	
12 nm	5.4	4.6	2.7	
15 nm	8.4	7.2	4.2	
20 nm	15.0	12.8	7.5	
60 nm	134.6	115.4	67.3	
Ab/nm²	0.012	0.010	0.006	

[Ab] pmol/cm²	2	1.7	0.98	

3.1. Indirect quantification through the analysis of the supernatant

Most quantification methods of antibody surface coverage rely on the indirect quantitation of unbound antibody remaining in the supernatant after adsorption to AuNP through common assays for protein quantification. In practice, excess unbound antibody in supernatant can be quantified with bicinchoninic acid (BCA) (Geng et al., 2016) or Bradford total protein assays (Filbrun and Driskell, 2016; Raoof et al., 2012; Ruiz et al., 2019; Tripathi and Driskell, 2018). Then the number of antibodies adsorbed on AuNP is deduced from the difference between the initial amount of antibody added to the AuNP suspension and the amount of unbound antibody that remained in the supernatant. However, antibody conjugation to AuNP is generally followed by a blocking step with another protein, typically BSA (De Mey et al., 1981; Hermanson, 2008a; Zhang et al., 2019a), to prevent aggregation of the nanoparticles in saline environment and to increase the long-term stability of the colloidal solution. BSA is also used to prevent the non specific binding and has proven to be much superior than PEG molecules (De Mey et al., 1981). This additional step, leading to the presence of another protein, makes the previous classical protein assays inapplicable. In this case, antibody assay in the supernatant still can be achieved by enzyme-linked immunosorbent assay (ELISA) using a microtiter plate coated with the corresponding antigen (Ben Haddada et al., 2017; Zhang et al., 2019a). Alternatively, prior to conjugation, antibody can be labeled with a fluorescent dye to achieve sufficient sensitivity of detection and unbound antibody in supernatant is measured by spectrofluorimetry at the excitation/emission wavelengths of the fluorescent dye (García-Fernández et al., 2017; Kumar et al., 2008).

Table 2: Indirect quantification of Ab/AuNP by the analysis of the supernatant

AuNP Diameter	Immobilization method	Quantification method	Ab/AuNP	Deviation *vs* theory (%)*	Reference
10 nm	Physisorption, pH 9 Physisorption, pH 4	Micro-BCA	20.4±0.5 19.9±3.7	434	(Geng et al., 2016)
15 nm	Physisorption, pH 8	FITC Fluorimetry ELISA	15±1.5 9.9±0.9	78 18	(Zhang et al., 2019b)
	Chemisorption, Traut Reagent	FITC Fluorimetry ELISA	13±1.4 6.9±0.7	55 ___	
17.2 nm	Chemisorption, carbohydrate oxidation+ SH	Alexa 488 Fluorimetry	8	___	(García-Fernández et al., 2017)
18 nm	Chemisorption, carbohydrate oxidation+ SH	Alexa 360, 594 Fluorimetry	9	___	(Kumar et al., 2008)
60 nm	Physisorption, pH 8	BioRad Protein assay	660±87	390	(Filbrun and Driskell,

					2016)
60 nm	Physisorption, pH 8 Protein A mediated	Bradford assay	227±35 68±10	69 ___	(Tripathi and Driskell, 2018)
60 nm	Physisorption, pH 7.5 Physisorption pH 8.5	BioRad Protein assay	240 ± 8 171 ± 11	78 27	(Ruiz et al., 2019)

* Calculated from the highest possible geometrical coverage

The Ab/AuNP ratios obtained following these methodologies are summarized in Table 2. Table 2 also contains the strategies employed for Ab immobilization and the deviation towards the max theoretical coverage estimated in Table 1 for a side-on orientation.

The data in Table 2 clearly point out an overestimation of the amount of Ab present on AuNP by the indirect strategies, up to 400 % overestimation when using total protein assays. The deviation is slightly lower using more specific techniques such as ELISA or fluorimetry. It should be noted that antibody quantification by these indirect methods assumes that no loss of antibody occurs during the purification process, *e.g.* during transfer of the solution from one container to another, or antibody adsorption to the container walls. Driskell and co-workers have estimated the loss of antibodies occurring during these steps and their optimization lowered the overestimation of antibody surface coverage on AuNP above 80 % (Filbrun and Driskell, 2016; Zhang et al., 2019b) vs (García-Fernández et al., 2017; Saha et al., 2014; Tripathi and Driskell, 2018; Welch et al., 2017).

3.2. Direct quantification through the analysis of Ab-AuNP bioconjugates

The most common and non invasive direct method for antibody adsorption on AuNP relies on the LSPR peak shift due to the local refractive index (RI) change caused by antibody adsorption (Iarossi et al., 2018; Pollitt et al., 2015). Although this approach provides a direct quantification of the adsorbed antibody, it requires accurate knowledge of RI of proteins on the nanoparticles surface. This is quite challenging because the RI depends on surface coverage, protein orientation and water content, none of which being constant (Bell et al., 2013; Vörös, 2004; Zhao et al., 2011). Other methods, like dynamic light scattering (DLS) and nanoparticle tracking analysis (NTA) measure the increase in hydrodynamic diameter after adsorption of protein on AuNP in order to derive information on surface coverages (Bell et al., 2013; Day et al., 2010; James and Driskell, 2013). However, the thickness of the bound protein layer does not directly provide accurate information of bound proteins. Some models had been derived allowing to correlate the average number of bound proteins to the hydrodynamic diameter increment, for instance, Taylor dispersion analysis (TDA) (Höldrich et al., 2017).

BCA protein assay (Liao and Hafner, 2005) and ELISA (Day et al., 2010; Hinterwirth et al., 2013; Tripathi and Driskell, 2018; Van Der Heide and Russell, 2016; Wang et al.,

2017) have also been used to directly quantify the adsorbed antibodies. However, even with some careful calibration treatment, *i.e.* removal of the contribution of nanoparticle by subtracting a spectrum of pure nanoparticle solution, overestimation of the antibody on nanoparticle was still obtained, demonstrating that nanoparticles interfere chemically and/or electromagnetically with assays (Liao and Hafner, 2005). Similar problems were encountered with fluorescence-based direct quantification of antibody in conjugates (Joshi et al., 2013).

To avoid the interference from the matrix, dissolution of nanoparticles or digestion of antibody strategies have been reported. The former method relies on the treatment of the Ab-AuNP bioconjugate by KI/I_2 mixture, followed by labeling of recovered antibody by the fluorescent dye NanoOrange and spectrofluorimetric measurement (Filbrun and Driskell, 2016). Similarly, another method based on quantification of the native fluorescence of proteins after dissolution of AuNP by KCN was reported afterwards (Kozlowski et al., 2018). The latter method is based on the complete digestion of the protein-AuNP conjugate in 6 N HCl followed by fluorescent labeling of the generated aminoacids and assay of glycine derivative by HPLC-fluorescence detection (Fountoulakis and Lahm, 1998). Of note, none of these methods are applicable to BSA-blocked Ab-AuNP bioconjugates.

Radioactive labeling of antibody has been reported as a robust method to quantify adsorbed antibody on planar surfaces and could be applied to AuNPs (Yoshimoto et al., 2010). However it requires the handling of radioactive material and is thus subjected to stringent restrictions.

Although different quantification methods are available, accurate quantification of surface coverage of antibody still remains challenging. We have recently introduced a fluorescence-based method to quantify antibody in bioconjugates. Briefly, prior to antibody adsorption to AuNP, a fluorophore tag (fluorescein isothiocyanate, FITC) was used to label the antibody. The final bioconjugates, *i.e.* AuNP-Ab(FITC) with free sites blocked by BSA, were treated with cyanide solution to dissolve the AuNP. Thus the interference from matrix was removed. Fluorescein was then quantified by spectrofluorimetry and the quantity of antibody was deduced. We have shown that this method is more accurate than the indirect ELISA and indirect fluorescence assay (Zhang et al., 2019b).

Table 3 summarizes the Ab/AuNP ratios obtained from the direct quantification methods and the strategies employed for Ab immobilization. Unlike the previous paragraph, the deviation towards the max theoretical coverage estimated in Table 1 was very low or inexistent as following these methodologies there is no overestimation, at least geometrically speaking, compared to theoretical coverages.

Table 3: Direct quantification of Ab/AuNP by the analysis of the AuNP-Ab bioconjugates

AuNP	Immobilization	Quantification method	Ab/AuNP	Reference

Diameter	method			
15 nm	Physisorption, pH 8 Chemisorption, Traut Reagent	AuNP Dissolution by NaCN + FITC then Fluorimetry	4.4±0.2 3.9±0.1	(Zhang et al., 2019b)
~ 30 nm	Chemisorption, OPSS-PEG-NHS	Reaction with HRP-IgG	33 - 55	(Day et al., 2010)
40 nm	Chemisorption, UV-activated (PIT)	λ shift calculations	40	(Iarossi et al., 2018)
52.6 nm	Physisorption, pH 8	λ shift calculations	65	(Pollitt et al., 2015)
60 nm	Physisorption, pH 8	AuNP Dissolution by KI/I_2 then Fluorimetry	309±93	(Filbrun and Driskell, 2016)

3.3. Conclusions of the section

In the preceding lines, we have presented the strategies for quantifying Ab coverage on AuNP and the results obtained by these strategies. Note that all the values for Ab/AuNP ratio given above correspond to the saturation coverage where the amount of antibodies is at its maximum, as often sought for biosensors applications. We did not discuss here strategies allowing for lowering this coverage down to 1Ab/AuNP suited for other applications such as targeted delivery (see ref (Montenegro et al., 2013) and references therein). The main conclusion is that analysis of the supernatant is often misleading and induces a considerable over-estimation of the bound Ab. The direct analysis of the bioconjugates is certainly more burdensome but provides more accurate coverages. These values must be put in perspective with the steric occupation of the surface by adsorbed antibodies, calculated here as if no hindrance is induced between adsorbed antibodies and therefore, slightly under-estimated. Most of these strategies do not allow for exploring the orientation of the antibodies on the surface than can be deduced from the accessibility of the recognition sites. In that respect, Protein A mediated adsorption on antibodies on 60 nm AuNPs decreased the Ab/AuNP by 70 % compared to simple physisorption (see data in Table 2 and refs. (García-Fernández et al., 2017; Saha et al., 2014; Tripathi and Driskell, 2018; Welch et al., 2017)), however the accessibility of antibodies and therefore their activity was improved to 91 % vs 23 % without Protein A. Therefore, the main objective when mastering AuNP-Ab bioconjugates engineering should be a perfect balance between coverage and accessibility.

4. Applications of Ab-AuNP bioconjugates in optical biosensing

Here we will present recent applications of Ab-AuNP bioconjugates based on the optical properties of AuNP, *i.e.* LSPR, Surface Enhanced Raman Scattering (SERS) and fluorescence enhancement or quenching/dequenching. The principle of these techniques is illustrated in Fig. 14 and a more detailed description of their principle can be found these reviews (Gauglitz, 2005; Guo, 2012; Le Ru and Etchegoin, 2009). According to the signal transduction type, the current well-developed immunoassays based on Ab-AuNP bioconjugates can be divided into four broad categories as depicted in Fig. 14: LSPR, propagating surface plasmon resonance (SPR), fluorescence, and SERS

immunoassay. For more detailed information about plasmonic biosensors, readers may refer to these recent reviews (Lee et al., 2018a; Liu et al., 2020).

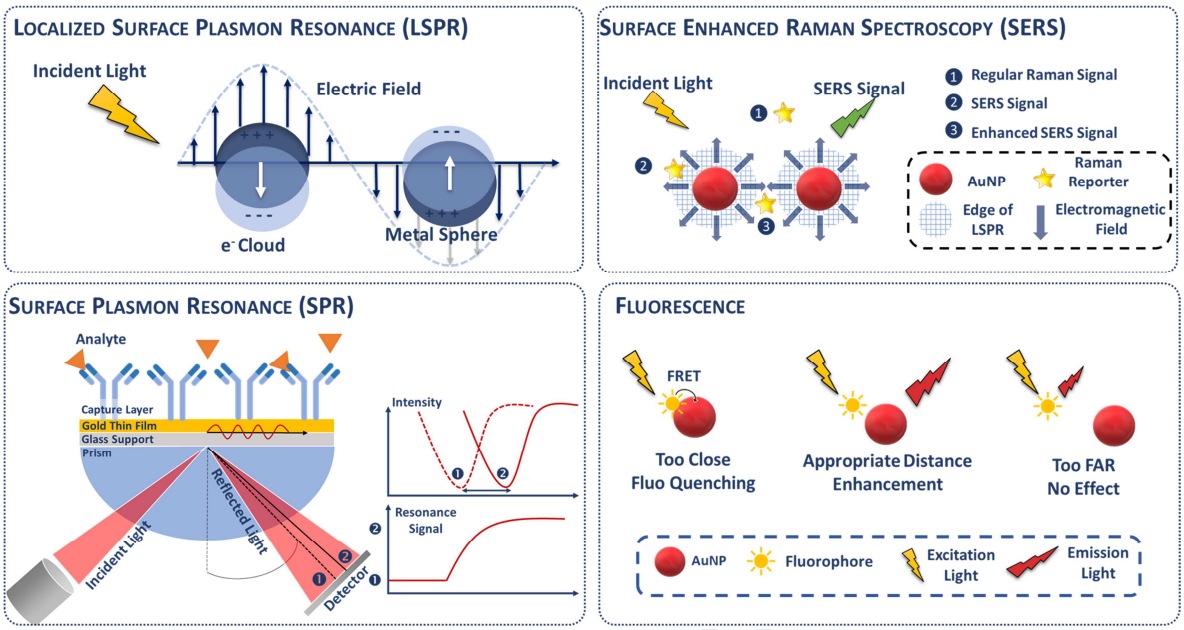

Fig. 14 : Readout and transduction techniques for Ab-AuNP bioconjugates-based biosensors: localized surface plasmon resonance (LSPR), propagating surface plasmon resonance (SPR), surface enhanced Raman scattering (SERS) and AuNP fluorescence enhancement and quenching.

4.1. Ab-AuNP bioconjugates in LSPR sensors

The general principle behind LSPR-based sensors is the LSPR peak shift arising from local refractive index (RI) change caused by binding event between Ab-AuNP and antigen or from antigen-induced crosslinking aggregation (Fig. 15). LSPR-based assays have been conducted both in homogeneous solution and on planar surfaces coated with AuNP monolayer.

For example, when Ab-AuNP binds to the target with only one epitope (Fig. 15A), the LSPR peak of AuNP red-shifts because of an increase of the RI close to AuNP. In addition, the peak shift is proportional to the target concentration. Thus, this assay is useful for quantitative detection (Englebienne, 1998; Englebienne et al., 2001). In the case where the target carries multiple binding sites (epitopes), the target acts as a linker and interparticle crosslinking-induced aggregation of AuNPs occurs (Fig. 15B) (Sepulveda et al., 2009). Moreover, the aggregation induces interparticle surface plasmon coupling of AuNPs, leading to the change of the absorbance spectrum and even to a color change of the colloidal solution. The degree of AuNP aggregation (or redispersion of aggregates) is proportional to the target concentration, thus allowing this assay to be useful in quantitative detection. For instance, the Ab-AuNP bioconjugates were applied to the detection of the food biotoxin staphylococcal enterotoxin A (SEA) (Ben Haddada et al., 2017), with a limit of detection (LOD) down to 5 ng/mL. Note that this assay was also done in milk, and despite the complexity of the matrix, no significant difference with the

response in buffer was observed, which suggests a good stability of the bioconjugate in complex media (Ben Haddada et al., 2017). The same bioconjugate was also used for naked-eye readout of SEA immunosensing through sandwich format and a similar LOD of 5 ng/mL was achieved in milk (Zhang et al., 2019a). Alternatively, a non-crosslinking aggregation of Ab-AuNP induced by an increasing salt concentration can be used as in ref. (Sharma et al., 2012), whereas the presence of antigen stabilized the colloidal solution.

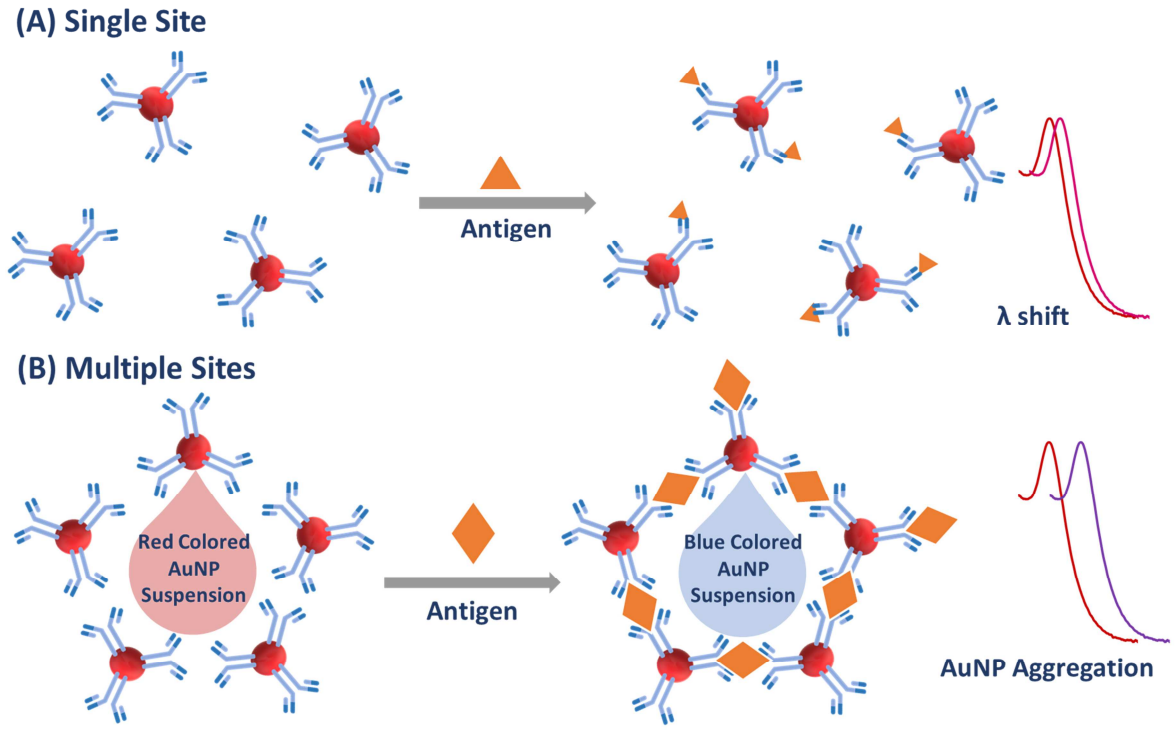

Fig. 15 : Schematic illustration of analyte-induced LSPR absorption change: (A) Local refractive index change inducing a small λ shift; (B) consequent λ shift due to analyte-induced crosslinking aggregation.

Other sensors based on LSPR peak shift have been fabricated by coating AuNPs onto a planar substrate surface. For example, AuNPs were attached to quartz (Frederix et al., 2003), ITO-glass (Lee et al., 2013), polystyrene (Inci et al., 2013), *etc*. Antibodies were then immobilized on AuNPs, consequently the sensing platform was employed to quantitatively detect antigens based on the LSPR peak shift which resulted from local RI change induced by target binding. These fabricated LSPR immunosensors showed high sensitivity and selectivity. For instance, the LOD of HIV-1 was estimated at 200 fg/mL (Lee et al., 2013), which is 70 fold better than that of a previously reported detection method (Chang et al., 2010). Inci et al. applied this technology for quantitative detection of intact virus in whole blood sample at clinically relevant concentrations (Inci et al., 2013).

4.2. Ab-AuNP bioconjugates for enhanced SPR sensors

AuNPs have been incorporated in SPR biosensors, providing an effective way to increase sensor response, which results from the optical coupling interaction of the propagating surface plasmons with localized surface plasmons of AuNPs. There are two different types: (i) AuNPs are immobilized on SPR sensor surface directly, and (ii) AuNPs are immobilized on top of the sensing layer (Fig. 16).

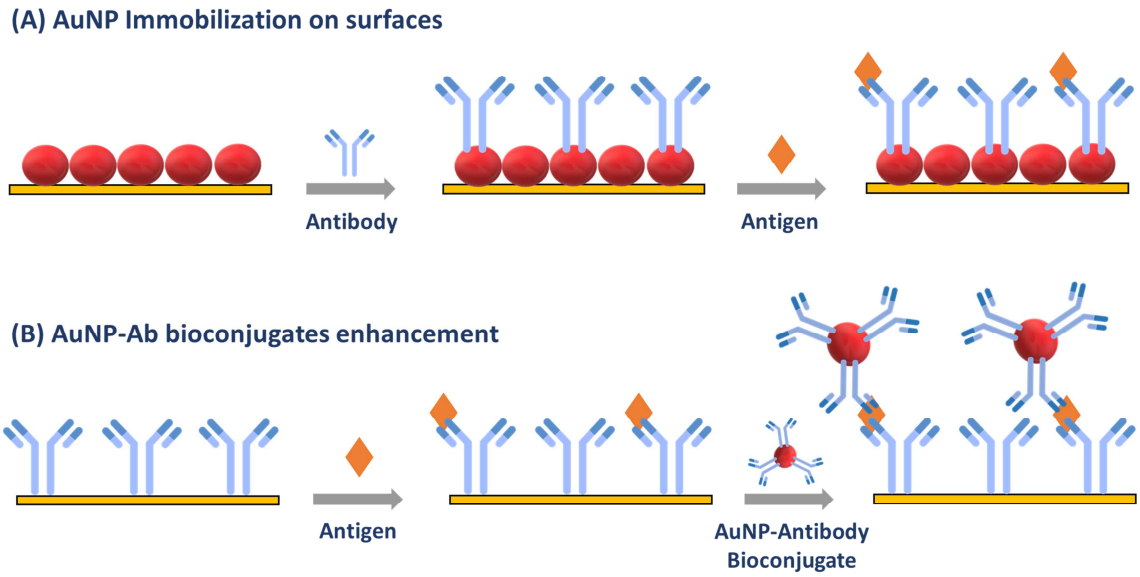

Fig. 16 : AuNP-based enhanced SPR sensors: (A) AuNPs are immobilized on SPR sensor surface directly; (B) AuNPs are immobilized on top of sensing layer.

For example, a layer of AuNPs was first created on SPR sensor surface, followed by another layer of Ab-AuNP. The two layers of AuNPs enhanced the sensitivity of the following detection of target (Wang et al., 2010). Alternatively, Ab-AuNP bioconjugates were bound at the last step forming a sandwich format (Fig. 16B). Briefly, a layer of capture antibody was immobilized on SPR sensor surface. After sample injection, Ab-AuNP finally bound to sensor surface. Signal amplification and lower LOD were obtained. This strategy has been applied to the detection of human IgG (Andrew Lyon et al., 1998), prostate-specific antigen (PSA) (Besselink et al., 2004; Choi et al., 2008; Uludag and Tothill, 2012) and carcinoembryonic antigen (CEA) (Špringer et al., 2017).

4.3. Ab-AuNP bioconjugates-based plasmon resonance scattering immunosensing

The light-scattering cross-section of an AuNP with a diameter of 60 nm is 200-300 times stronger than that of a polystyrene bead of same size, and 4-5 orders of magnitude stronger than that of a fluorescent dye, *e.g.*, fluorescein (Lee and El-Sayed, 2006; Yguerabide and Yguerabide, 1998). On the other hand, dynamic light scattering (DLS) is a technique routinely used to analyze the size and size distribution of nanoparticles. Combining the use of AuNP as light scattering enhancer and DLS as read-out provides a useful sensor design.

In practice, when Ab-AuNP bioconjugates are mixed with a sample containing the target, depending on its concentration, the target binding will cause AuNPs to form dimers, oligomers, or aggregates. The relative ratio of different forms can be measured quantitatively through DLS analysis. This ratio increases accordingly with increased amount of antigen in sample, and such a correlation forms the analytical basis of a homogeneous immunoassay. By exploiting this sensing platform, human IgG (Jans et al., 2009), PSA (Liu et al., 2008; Mustafaoglu et al., 2017) and influenza A (H1N1) virus (Lai et al., 2015) have been quantified. The homogeneous assay does not involve any washing step and yields highly sensitive, specific and rapid results. Moreover, extremely small amounts of samples are needed for the assay. Recently, a sandwich-based homogeneous immunosensor based on the plasmonic resonance energy transfer phenomenon between AuNP- and QD-anti-PSA conjugates allowed the quantification of PSA down to 0.2 fM by scattering intensity measurement at the single molecule level with a dark field microscope setup (Liu et al., 2019).

4.4. Ab-AuNP bioconjugates-based fluorescence immunosensing

AuNP can lead to both fluorophore quenching or enhancement which can be explained by the well-established Förster resonance energy transfer (FRET) mechanism (Clegg, 1995) (as shown in Fig. 14). When AuNP and fluorophore are close to each other, FRET occurs from the fluorophore to AuNP and thus quenching happens (Schneider et al., 2006). In contrast, at an appropriate distance to AuNP, fluorescence enhancement can happen, which is typically referred to as plasmon-enhanced fluorescence (PEF) (Aslan et al., 2005). Specially, Anger et al. (Anger et al., 2006) theoretically and experimentally investigated the relationship between the fluorescence rate and the distance between AuNP and fluorophore and demonstrated a continuous transition from fluorescence enhancement to fluorescence quenching of a single molecule on an AuNP.

Generally, a AuNP-based fluorescence probe system consists of two functional components: the recognition element, here antibody, which provides specific binding of target; and the fluorescent dye, which is used to analyze the binding event. The high loading efficiency of the fluorescent dye on AuNP surface with high area-to-volume ratio and high fluorescence enhancement or quenching/unquenching abilities of the fluorescent dye-AuNP pairs make this probe ultrasensitive. Assays are typically designed as fluorescence-nanoprobe labeling and analyte-induced fluorescence quenching/dequenching (recovery).

Alternative assay platforms, for instance, fiber-optic biosensors based on AuNP-fluorescent dye enhancement, have been described by different research groups (Chang et al., 2010; Hong and Kang, 2006; Hsieh et al., 2007). Briefly, a capture antibody is immobilized on the surface of an optical fiber. After sample injection, a fluorescence probe consisting of fluorophore-labeled antibody conjugated AuNP *via* protein A is added. Subsequently, the fluorescence signal is generated and measured by the photomultiplier tube (Fig. 17). In this assay, two factors were considered to enhance the assay sensitivity. First, the electromagnetic field around the AuNP surface efficiently

enhanced the fluorescence signal. Second, there were multiple fluorophores on each AuNP allowing several fluorophores to be simultaneously excited during measurement. These two effects combine to produce a significant improvement in the sensitivity of the system compared to a conventional fluorescence probe or ELISA.

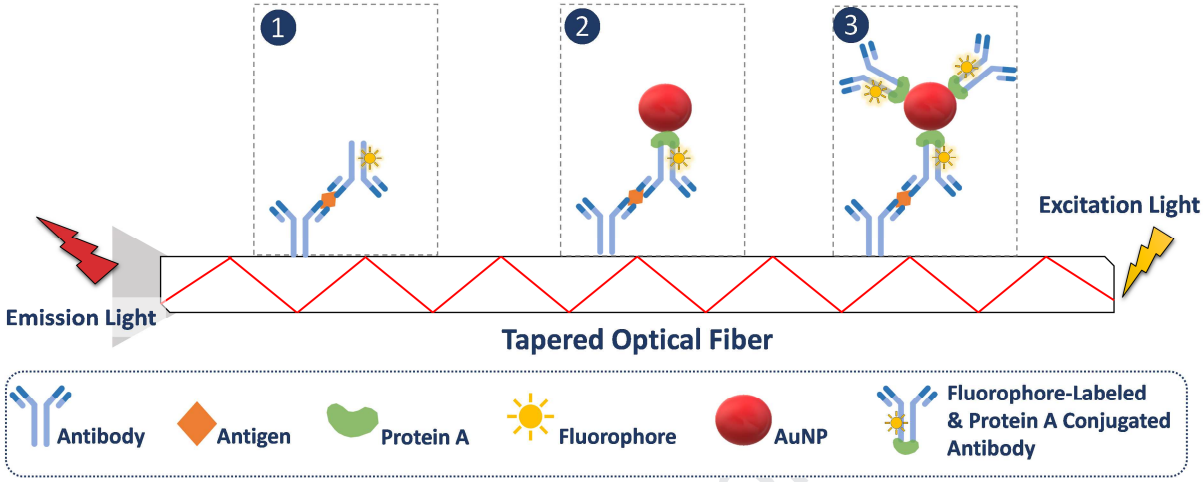

Fig. 17 : Schematic diagrams of fluorescence-based biosensor formats: (1) regular immunosensing with fluorophore-labeled antibody; (2) immunosensing using AuNP as fluorescence enhancer; (3) immunosensing using AuNP with several fluorophores. Picture is adapted from ref. (Hong and Kang, 2006).

Based on the latter dequenching format, porcine reproductive and respiratory syndrome virus was detected (Stringer et al., 2008). A fluorophore-labeled antibody was immobilized on protein A-modified AuNP. In such case, the fluorescence was quenched by AuNP. Upon binding of antigen, conformational change within the immune complex increased the distance between the fluorescent dye and AuNP, leading to a dequenching/recovery effect.

Liu et al. also introduced a new AuNP-based fluorescence-activable probe for immunosensing ultralow levels of PSA in patient serum samples at pg/mL level (Fig. 18) (Liu et al., 2013). Thousands of fluorescent dye molecules (rhodamine B isothiocyanate) were loaded on each AuNP. Then the dye layer was covered with detection antibody through electrostatic interactions. In the presence of PSA in serum samples, the AuNP-dye-antibody probes were captured onto the PS plate *via* sandwich format. Until this stage the fluorescence of dye was highly quenched by AuNP. Upon addition of cysteamine into detection system, the fluorescent dyes were competitively displaced by cysteamine from the AuNP surface, leading to significant recovery of fluorescence. Thus, the concentration of PSA in serum samples could be quantified according to the intensity of the recovered fluorescence. The assay LOD using this developed probe was more than 2 orders of magnitude lower compared to the assay using rhodamine-labeled detection antibody.

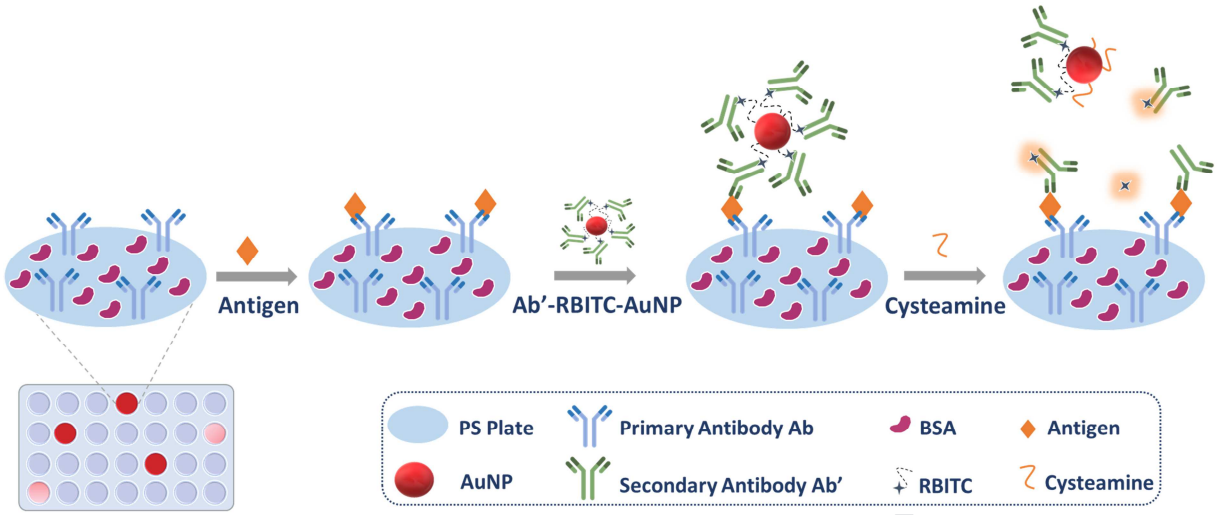

Fig. 18 : Schematic illustration of dequenching of fluorescent dyes. Picture is adapted from ref. (Liu et al., 2013).

Ab-AuNP bioconjugates are not often used as fluorescence immunosensors for LFA devices because of the quenching effect of AuNPs. However, silica coating of AuNPs can prevent this quenching, and an LFA assay was built up for the quantitation of hTSH (Preechakasedkit et al., 2018). Its principle relies on core-shell AuNP@SiO_2 decorated with Eu(III) chelates and anti-hTSH antibody combined with naked eye or fluorimetric readout with a smartphone. Naked eye readout sensitivity was improved by a factor of 5 compared to simple AuNP-Ab conjugate.

4.5. Ab-AuNP bioconjugates-based SERS immunosensing

SERS is a powerful spectroscopic technique that provides *in-situ* nondestructive fingerprint information. More importantly, its ultrahigh signal enhancement (up to 10^{14}) makes it capable of single-molecule detection. The principle of AuNP-based SERS sensing relies on the excitation of the LSPR of AuNP resulting in a large electromagnetic field localized at AuNP surface. This property is exploited to measure enhanced vibrational molecular signatures. SERS nanoprobes have been widely applied in immunoassays. As the probe, the essential design is the use of AuNP with antibody and Raman reporter molecules. The total enhancement factor results from (i) LSPR-enhanced Raman scattering and (ii) chemical enhancement factor. The assays are typically designed as optical SERS-nanoprobes and analyte-induced SERS nanoprobe aggregation/anti-aggregation formats.

Using SERS nanoprobes as optical labels Grubisha et al. reported a sandwich format immunoassay for detection of PSA. To prepare the Raman probe, AuNP was functionalized with a monolayer of intrinsically strong Raman reporter (DSNB, Fig. 5) followed by coating a layer of antibody (Grubisha et al., 2003). In this case, the distance between the Raman reporter and the AuNP surface was minimal and the number of the Raman-reporters on each AuNP was maximized. These two factors led to an enhanced

sensitivity of this assay. All the same, Lee et al. have applied this sandwich format coupled to a Raman probe but they used multi-valent antibodies to enhance the sensitivity of SERS detection by a factor of 100 compared to classical antibodies (Lee et al., 2018b). The signal of SERS nanoprobe was further amplified by combining graphene oxide (GO) (Fu et al., 2019). This combination brought two advantages. The first is that one GO sheet can carry a lot of detection antibodies. The second is that the distance of functionalized AuNPs was shortened which resulted in hot spots. The analytical performance of this strategy was improved by 100 times compared to the one only using antibody/Raman reporter-AuNPs in detection of cardiac troponin I. In a similar line, a sandwich-format immunosensor including Ab-AuNP decorated with ATP reporters as SERS nanoprobe and 2D gold trisoctahedron superlattice substrate was set up to quantify rabbit IgG with a low limit of detection of 1 pg/mL (Dong et al., 2018).

To improve the stability of SERS nanoprobe, other core-shell immunoprobes were developed. AuNPs, after labeling by Raman reporter, were coated with a metal layer either Au (Wan et al., 2017) or Ag (Li et al., 2014; Wang et al., 2016; Xie et al., 2015) prior to antibody immobilization. This thin shell prevented the dissociation of Raman reporter and its non-specific interactions with co-existing antibody in complex biological medium. Thus the sensitivity of the immunoprobe was improved.

For instance, Xie et al. exploited an immunochromatographic assay (ICA) based on core-shell immunoprobe for ultrasensitive and quantitative detection of clenbuterol (Fig. 19) (Xie et al., 2015). The principle of this assay is similar to conventional ICA based on AuNP but using a SERS probe which consisted of Au@Ag core-shell nanoparticles labeled Raman reporter (4-mercaptobenzoic acid, MBA) and antibody (Au^{MBA}@Ag-Ab). After the ICA procedure, the specific Raman scattering intensity of MBA on the test line was measured for quantitative detection of clenbuterol. The LOD of this assay was improved by 2-3 orders of magnitude compared to other immunoassays. More recently Xiao et al. applied this same principle to detect the avian influenza A (H7N9) virus with a sensitivity 3 orders of magnitude higher than the corresponding hemagglutination assay (Xiao et al., 2019).

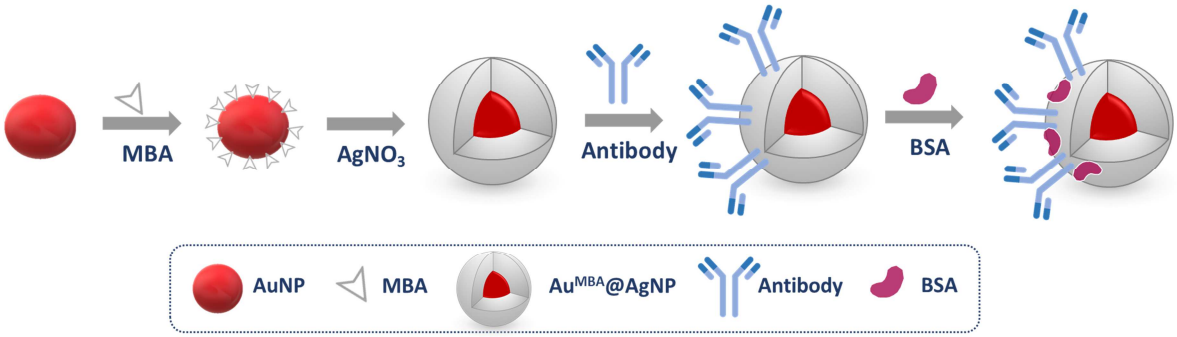

Fig. 19 : Preparation of SERS nanoprobe: Au^{MBA}@Ag-Ab. Picture is adapted from ref. (Xie et al., 2015).

Qian et al. successfully applied pegylated SERS nanoprobe for cancer cell detection (Qian et al., 2008). Large optical enhancement was achieved under *in vivo* conditions for tumor detection in live animals. Similarly, Cho et al. applied it for the isolation and analysis of circulating cancer stem cells through Raman imaging based on SERS nanoprobes (Cho et al., 2018).

Another assay format is based on antigen-induced aggregation/anti-aggregation of SERS nanoprobes. Wang et al. reported the application of SERS nanoprobes in target-induced aggregation assay (Wang et al., 2013). In the system, there were two SERS nanoprobes, spherical AuNP and gold nanorod (AuNR). Both were decorated with Raman reporter and half-antibody fragments (as shown in Fig. 20). In the presence of target, the SERS nanoprobes aggregated leading to strong SERS enhancement arising from plasmonic coupling, and SERS spectra were acquired directly on the sample solution. Instead, after the SERS nanoprobes reacted with target, the aggregated nanoparticles were captured and concentrated through a membrane filter. SERS analysis was acquired from the surface of the membrane (Filbrun et al., 2017; Lopez et al., 2016).

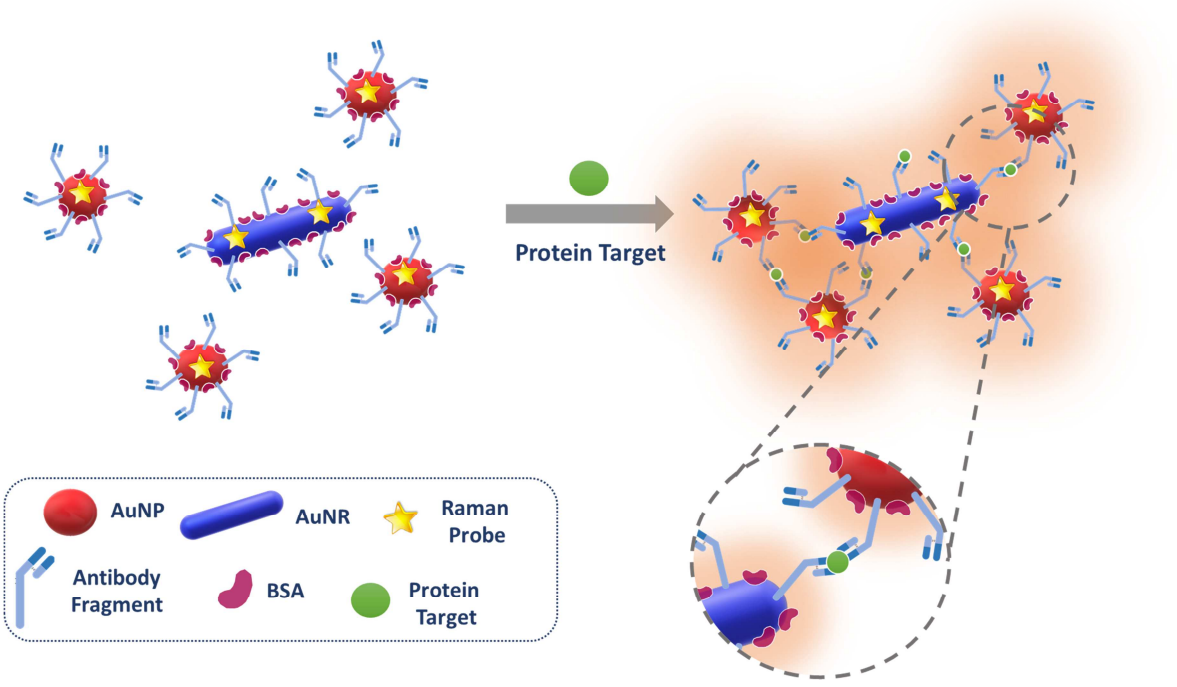

Fig. 20 : Schematic illustration of single-step SERS immunoassay *via* target-controlled assembly of SERS nanoprobes. Picture is adapted from ref. (Wang et al., 2013).

Wu et al. exploited a SERS immunoassay in anti-aggregation format for ultrasensitive detection of folic acid (FA) based on gold and silver nanoparticles (AuNP–AgNP) heterodimers (Fig. 21) (Wu et al., 2016). In practice, the AuNP was coated with anti-FA antibody and Raman reporter (4-aminothiophenol (4-ATP)); AgNP was coated with antigen (FA-BSA conjugate) and Raman reporter (4-ATP). Without target in sample, the AuNP-Ab/Raman reporters and the AgNP-FA/Raman reporters assembled and formed

AuNP-AgNP heterodimers with high yield through antibody-antigen recognition. Because of the strong optical coupling and intense hot spots between heterodimers, the colloidal solution exhibited strong SERS intensity. However, upon addition of free FA, it competed with the AgNP-labeled FA for binding to Ab-AuNP. Thus the amount of heterodimers decreased and the SERS intensity was reduced. Furthermore, the concentration of target FA was quantified through Raman intensity. The LOD of FA was down to 0.86 pg/mL, and this method also was applied successfully in human serum samples.

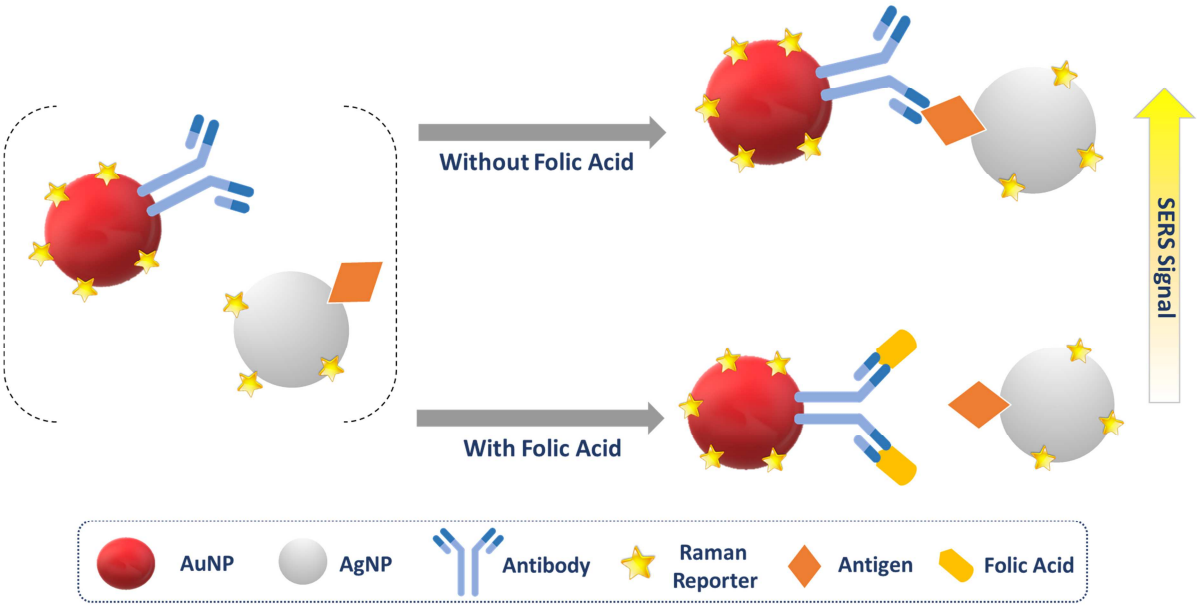

Fig. 21 : Schematic illustration of the SERS immunoassay for detection of folic acid (FA) based on AuNP−AgNP heterodimers formation. Picture is adapted from ref. (Wu et al., 2016).

Besides the applications in optical biosensing mentioned above, Ab-AuNP bioconjugates have also been used in combination with other transduction techniques, for example, piezoelectric transduction using QCM-D. The sensing design is the same as for AuNP-enhanced SPR sensor and the incorporation of AuNPs into QCM-based sensing systems enhanced detection sensitivity owing to their high surface area (Ben Haddada et al., 2016; Ben Haddada et al., 2018; Makaraviciute et al., 2014) and as mass enhancer (Chu et al., 2006; Jin et al., 2009).

5. Conclusions and perspectives

Here, we have reviewed the literature data on antibody-gold nanoparticle bioconjugates for biosensors, with a focus on IgG-type antibodies and spherical AuNPs, from their design to their characterization and up to their application in optical biosensing. The first part of this review comprehensively covered the existing methodologies allowing for engineering Ab-AuNP bioconjugates *via* physisorption and chemisorption. This section provides the reader with the pros and cons of each method and with guidance in choosing the adapted protocol to achieve the desired bioconjugate. In the second part,

we investigated the challenging question of the quantification of antibodies on AuNPs surface through direct and indirect strategies. Through a critical restitution we have addressed the relevant strategies and rationalized the literature results with respect to the IgG structure and the geometrical constraints. Often over-estimated, antibodies coverage quantification remains a key-factor for biosensors efficiency. The third and last part of this review informed on the potential of these bioconjugates for optical biosensing. The excellent optical properties of AuNP related to LSPR allowing various signal transduction approaches, have contributed to the development of easy-to-use, rapid, low-cost immunoassays including Ab-AuNP conjugates. Optimization of bioconjugation for the sensing systems is still required to meet the demands of clinical diagnostics in complex biological fluids such as urine, serum, and blood. For example, further miniaturization of antibody allows increment of binding sites on AuNP surface for a better sensitivity. Assays can be further integrated into mobile phones or computers for quantitative real-time monitoring. The fundamental advantages of AuNP will arguably contribute to the development of immunosensors in the following years.

Acknowledgement

This work was supported by French state funds managed by the ANR within the Investissements d'Avenir programme under reference ANR-11-IDEX-0004-02, and more specifically within the framework of the Cluster of Excellence MATISSE led by Sorbonne Universités. This work was also supported by the ANR grant ChirOptMol (No. ANR-18-CE09-0010). LZ. also thanks the Sorbonne Université – Nanyang Technological University Dual Degree PhD programme for scholarship funding.

Abbreviations used: 4-ATP, 4-aminothiophenol; Ab, antibody; AMBH, 2-acetamido-4-mercaptobutyric acid hydrazide; BCA, bicinchoninic acid; BSA, bovine serum albumin; NP, nanoparticle; CEA, carcinoembryonic antigen; DLS, dynamic light scattering; DSNB, 5,5'-dithobis(succinimidyl-2-nitrobenzoate); DSP, 3,3'-dithiobis(succinimidyl propionate); DTSSP, 3,3'-dithiobis(sulfosuccinimidyl propionate); DTT, dithiothreitol; EDC, ethyl diisopropylcarbodiimide; ELISA, enzyme-linked immunosorbent assay; FA, folic acid; FITC, fluorescein isothiocyanate; ICA, immunochromatographic assay; IgG, immunoglobulin G; LFA, lateral flow assay; LC-SPDP, N-succinimidyl 6-(3-(2-pyridyldithio)propionamido)hexanoate; LOD, limit of detection; LSPR, localized surface plasmon resonance; MBA, 4-mercaptobenzoic acid; MEA, 2-mercaptoethylamine; NBS, nucleotide binding site; NHS, N-hydroxysuccinimide; NTA, nanoparticle tracking analysis; PEF, plasmon enhanced fluorescence; PEG, poly(ethylene glycol); PIT, photochemical immobilization technique; PSA, prostate specific antigen; QCM, quartz crystal microbalance; RI, refractive index; SATA, N-succinimidyl S-acetylthioacetate; SATP, N-succinimidyl S-acetylthiopropionate; SAV, streptavidin; SEA, staphylococcal enterotoxin A; SERS, surface enhanced Raman scattering; SPDP, N-succinimidyl 3-(2-pyridyldithio)propionate; TCEP, tris(2-carboxyethyl-phosphine)

References

Aldewachi, H., Chalati, T., Woodroofe, M., Bricklebank, N., Sharrack, B., Gardiner, P., 2018. Nanoscale 10(1), 18-33.
Alves, N.J., Kiziltepe, T., Bilgicer, B., 2012. Langmuir 28(25), 9640-9648.
Andrew Lyon, L., Musick, M.D., Natan, M.J., 1998. Anal. Chem. 70(24), 5177-5183.
Anger, P., Bharadwaj, P., Novotny, L., 2006. Phys. Rev. Lett. 96(11), 3-6.
Aslan, K., Gryczynski, I., Malicka, J., Matveeva, E., Lakowicz, J.R., Geddes, C.D., 2005. Curr. Opin. Biotechnol. 16(1), 55-62.
Bagchi, P., Birnbaum, S.M., 1981. J. Colloid Interface Sci. 83(2), 460-478.
Balevicius, Z., Ramanaviciene, A., Baleviciute, I., Makaraviciute, A., Mikoliunaite, L., Ramanavicius, A., 2011. Sens. Actuators B 160(1), 555-562.
Bell, N.C., Minelli, C., Shard, A.G., 2013. Anal. Methods. 5(18), 4591-4601.
Ben Haddada, M., Huebner, M., Casale, S., Knopp, D., Niessner, R., Salmain, M., Boujday, S., 2016. J. Phys. Chem. C 120(51), 29302-29311.
Ben Haddada, M., Hu, D., Salmain, M., Zhang, L., Peng, C., Wang, Y., Liedberg, B., Boujday, S., 2017. Anal. Bioanal. Chem. 409(26), 6227-6234.
Ben Haddada, M., Salmain, M., Boujday, S., 2018. Sens. Actuators B 255, 1604-1613.
Besselink, G.A.J., Kooyman, R.P.H., van Os, P.J.H.J., Engbers, G.H.M., Schasfoort, R.B.M., 2004. Anal. Biochem. 333(1), 165-173.
Bewley, T.A., Li, C.H., 1969. Int. J. Prot. Res. 1(1-4), 117-124.
Biju, V., 2014. Chem. Soc. Rev. 43(3), 744-764.
Boujday, S., Bantegnie, A., Briand, E., Marnet, P.-G., Salmain, M., Pradier, C.-M., 2008. J. Phys. Chem. B 112(21), 6708-6715.
Boujday, S., Méthivier, C., Beccard, B., Pradier, C.-M., 2009. Anal. Biochem. 387(2), 194-201.
Boujday, S., Parikh, A.N., Liedberg, B., Song, H., 2017. Functionalisation of Gold Nanoparticles, in: Louis, C., Pluchery, O. (Eds.), Gold Nanoparticles for Physics, Chemistry and Biology. World Scientific, pp. 201-227.
Bragg, P.D., Hou, C., 1980. Eur. J. Biochem. 106(2), 495-503.
Burns, J.A., Butler, J.C., Moran, J., Whitesides, G.M., 1991. J. Org. Chem 56(8), 2648-2650.
Byzova, N.A., Safenkova, I.V., Slutskaya, E.S., Zherdev, A.V., Dzantiev, B.B., 2017. Bioconjugate Chem. 28(11), 2737-2746.
Carter, T., Mulholland, P., Chester, K., 2016. Immunotherapy 8(8), 941-958.
Chang, Y.F., Wang, S.F., Huang, J.C., Su, L.C., Yao, L., Li, Y.C., Wu, S.C., Chen, Y.M.A., Hsieh, J.P., Chou, C., 2010. Biosens. Bioelectron. 26(3), 1068-1073.
Cho, H.-Y., Hossain, M.K., Lee, J.-H., Han, J., Lee, H.J., Kim, K.-J., Kim, J.-H., Lee, K.-B., Choi, J.-W., 2018. Biosens. Bioelectron. 102, 372-382.
Choi, J.W., Kang, D.Y., Jang, Y.H., Kim, H.H., Min, J., Oh, B.K., 2008. Colloids Surf. A 313-314, 655-659.
Chu, X., Zhao, Z.-L., Shen, G.-L., Yu, R.-Q., 2006. Sens. Actuators B 114(2), 696-704.
Ciaurriz, P., Fernández, F., Tellechea, E., Moran, J.F., Asensio, A.C., 2017. Beilstein J. Nanotechnol. 8(1), 244-253.
Clegg, R.M., 1995. Curr. Opin. Biotechnol. 6(1), 103-110.
Das, A., Soehnlen, E., Woods, S., Hegde, R., Henry, A., Gericke, A., Basu, S., 2011. J. Nanopart. Res. 13(12), 6283-6290.
Day, E.S., Bickford, L.R., Slater, J.H., Riggall, N.S., Drezek, R.A., West, J.L., 2010. Int. J. Nanomed. 5(1), 445-454.
De Mey, J., Moeremans, M., Geuens, G., Nuydens, R., De Brabander, M., 1981. Cell Biol. Int. Rep. 5(9), 889-899.

Della Ventura, B., Schiavo, L., Altucci, C., Esposito, R., Velotta, R., 2011. Biomed. Opt. Express 2(11), 3223-3231.
Demanèche, S., Chapel, J.-P., Monrozier, L.J., Quiquampoix, H., 2009. Colloids Surf. B 70(2), 226-231.
Dong, D., Yap, L.W., Smilgies, D.M., Si, K.J., Shi, Q., Cheng, W., 2018. Nanoscale 10(11), 5065-5071.
Duncan, R.J.S., Weston, P.D., Wrigglesworth, R., 1983. Anal. Biochem. 132(1), 68-73.
Eck, W., Craig, G., Sigdel, A., Ritter, G., Old, L.J., Tang, L., Brennan, M.F., Allen, P.J., Mason, M.D., 2008. ACS Nano 2(11), 2263-2272.
El-Sayed, I.H., Huang, X., El-Sayed, M.A., 2005. Nano Lett. 5(5), 829-834.
Englebienne, P., 1998. Analyst 123(7), 1599-1603.
Englebienne, P., Van Hoonacker, A., Verhas, M., 2001. Analyst 126(10), 1645-1651.
Faraday, M., 1857. Philos. Trans. R. Soc. London 147, 145-181.
Ferrari, E., Darios, F., Zhang, F., Niranjan, D., Bailes, J., Soloviev, M., Davletov, B., 2010. J. Nanobiotechnol. 8(1), 9.
Filbrun, S.L., Driskell, J.D., 2016. Analyst 141(12), 3851-3857.
Filbrun, S.L., Filbrun, A.B., Lovato, F.L., Oh, S.H., Driskell, E.A., Driskell, J.D., 2017. Analyst 142(23), 4456-4467.
Finetti, C., Sola, L., Pezzullo, M., Prosperi, D., Colombo, M., Riva, B., Avvakumova, S., Morasso, C., Picciolini, S., Chiari, M., 2016. Langmuir 32(29), 7435-7441.
Fountoulakis, M., Lahm, H.-W., 1998. J. Chromatog. A 826(2), 109-134.
Frederix, F., Friedt, J.-M., Choi, K.-H., Laureyn, W., Campitelli, A., Mondelaers, D., Maes, G., Borghs, G., 2003. Anal. Chem. 75(24), 6894-6900.
Fu, X., Wang, Y., Liu, Y., Liu, H., Fu, L., Wen, J., Li, J., Wei, P., Chen, L., 2019. Analyst 144(5), 1582-1589.
García-Fernández, L., Garcia-Pardo, J., Tort, O., Prior, I., Brust, M., Casals, E., Lorenzo, J., Puntes, V.F., 2017. Nanoscale 9(18), 6111-6121.
Gauglitz, G., 2005. Anal. Bioanal. Chem. 381(1), 141-155.
Geng, S.B., Wu, J., Alam, M.E., Schultz, J.S., Dickinson, C.D., Seminer, C.R., Tessier, P.M., 2016. Bioconjugate Chem. 27(10), 2287-2300.
Geoghegan, W.D., Ackerman, G.A., 1977. J. Histochem. Cytochem. 25(11), 1187-1200.
Geoghegan, W.D., 1988. J. Histochem. Cytochem. 36(4), 401-407.
Ghosh, B.K., Ghosh, A., 1984. J. Bacteriol. 159(2), 668-677.
Grubisha, D.S., Lipert, R.J., Park, H.-Y., Driskell, J., Porter, M.D., 2003. Anal. Chem. 75(21), 5936-5943.
Guo, X., 2012. J. Biophotonics 5(7), 483-501.
Haller, E., Lindner, W., Lämmerhofer, M., 2015. Anal. Chim. Acta 857, 53-63.
Harris, L.J., Larson, S.B., Hasel, K.W., McPherson, A., 1997. Biochemistry 36(7), 1581-1597.
Harris, L.J., Skaletsky, E., McPherson, A., 1998. J. Mol. Biol. 275(5), 861-872.
Hazarika, P., Ceyhan, B., Niemeyer, C.M., 2005. Small 1(8-9), 844-848.
Hermanson, G.T., 2008a. Preparation of Colloidal Gold-Labeled Proteins, in: Hermanson, G.T. (Ed.) Bioconjugate Techniques (Second Edition). Academic Press, New York, pp. 924-935.
Hermanson, G.T., 2008b. Antibody Modification and Conjugation, in: Hermanson, G.T. (Ed.) Bioconjugate Techniques (Second Edition). Academic Press, New York, pp. 783-823.
Hermanson, G.T., 2008c. Functional Targets, in: Hermanson, G.T. (Ed.) Bioconjugate Techniques (Second Edition). Academic Press, New York, pp. 1-168.

Hermanson, G.T., 2008d. Fluorescent Probes, in: Hermanson, G.T. (Ed.) Bioconjugate techniques (Second Edition). Academic Press, New York, pp. 396-497.
Hinterwirth, H., Stübiger, G., Lindner, W., Lämmerhofer, M., 2013. Anal. Chem. 85(17), 8376-8384.
Höldrich, M., Liu, S., Epe, M., Lämmerhofer, M., 2017. Talanta 167, 67-74.
Hong, B., Kang, K.A., 2006. Biosens. Bioelectron. 21(7), 1333-1338.
Hook, F., Rodahl, M., Kasemo, B., Brzezinski, P., 1998. Proc. Natl Acad. Sci. 95(21), 12271-12276.
Horisberger, M., Rosset, J., Bauer, H., 1975. Experientia 31(10), 1147-1149.
Horisberger, M., Rosset, J., 1977. J. Histochem. Cytochem. 25(4), 295-305.
Horisberger, M., Clerc, M.F., 1985. Histochem. 82(3), 219-223.
Hsieh, B.-Y., Chang, Y.-F., Ng, M.-Y., Liu, W.-C., Lin, C.-H., Wu, H.-T., Chou, C., 2007. Anal. Chem. 79(9), 3487-3493.
Hsu, Y.-H., 1984. Anal. Biochem. 142(1), 221-225.
Iarossi, M., Schiattarella, C., Rea, I., De Stefano, L., Fittipaldi, R., Vecchione, A., Velotta, R., Ventura, B.D., 2018. ACS Omega 3(4), 3805-3812.
Inci, F., Tokel, O., Wang, S., Gurkan, U.A., Tasoglu, S., Kuritzkes, D.R., Demirci, U., 2013. ACS Nano 7(6), 4733-4745.
Jain, P.K., Lee, K.S., El-Sayed, I.H., El-Sayed, M.A., 2006. J. Phys. Chem. B 110(14), 7238-7248.
James, A.E., Driskell, J.D., 2013. Analyst 138(4), 1212-1218.
Jans, H., Liu, X., Austin, L., Maes, G., Huo, Q., 2009. Anal. Chem. 81(22), 9425-9432.
Jin, X., Jin, X., Chen, L., Jiang, J., Shen, G., Yu, R., 2009. Biosens. Bioelectron. 24(8), 2580-2585.
Joshi, P.P., Yoon, S.J., Hardin, W.G., Emelianov, S., Sokolov, K.V., 2013. Bioconjugate Chem. 24(6), 878-888.
Jung, Y., Lee, J.M., Jung, H., Chung, B.H., 2007. Anal. Chem. 79(17), 6534-6541.
Kao, H.-W., Lin, Y.-Y., Chen, C.-C., Chi, K.-H., Tien, D.-C., Hsia, C.-C., Lin, M.-H., Wang, H.-E., 2013. Bioorg. Med. Chem. Lett. 23(11), 3180-3185.
Karyakin, A.A., Presnova, G.V., Rubtsova, M.Y., Egorov, A.M., 2000. Anal. Chem. 72(16), 3805-3811.
Kelly, K.L., Coronado, E., Zhao, L.L., Schatz, G.C., 2003. J. Phys. Chem. B 107(3), 668-677.
Kozlowski, R., Ragupathi, A., Dyer, R.B., 2018. Bioconjugate Chem. 29(8), 2691-2700.
Kumar, S., Aaron, J., Sokolov, K., 2008. Nature Prot. 3(2), 314-320.
Lai, Y.H., Koo, S., Oh, S.H., Driskell, E.A., Driskell, J.D., 2015. Anal. Methods. 7(17), 7249-7255.
Le Ru, E., Etchegoin, P., 2009. Principles of Surface-Enhanced Raman Spectroscopy: And Related Plasmonic Effects. Elsevier B.V., Amsterdam.
Lee, J.-H., Cho, H.-Y., Choi, H.K., Lee, J.-Y., Choi, J.-W., 2018a. Int. J. Mol. Sci. 19(7), 2021-2034.
Lee, J.H., Kim, B.C., Oh, B.K., Choi, J.W., 2013. Nanomedicine 9(7), 1018-1026.
Lee, K.S., El-Sayed, M.A., 2006. J. Phys. Chem. B 110(39), 19220-19225.
Lee, M., Kim, H., Kim, E., Yi, S.Y., Hwang, S.G., Yang, S., Lim, E.-K., Kim, B., Jung, J., Kang, T., 2018b. ACS Appl. Mater. Interfaces 10(44), 37829-37834.
Leggett, R., Lee-Smith, E.E., Jickells, S.M., Russell, D.A., 2007. Angew. Chem. Int. Ed. 46(22), 4100-4103.
Li, M., Yang, H., Li, S., Zhao, K., Li, J., Jiang, D., Sun, L., Deng, A., 2014. J. Agr. Food Chem. 62(45), 10896-10902.
Li, Y., Schluesener, H.J., Xu, S., 2010. Gold Bull. 43(1), 29-41.

Liao, H., Hafner, J.H., 2005. Chem. Mat. 17(18), 4636-4641.
Lim, C.Y., Owens, N.A., Wampler, R.D., Ying, Y., Granger, J.H., Porter, M.D., Takahashi, M., Shimazu, K., 2014. Langmuir 30(43), 12868-12878.
Liu, D., Huang, X., Wang, Z., Jin, A., Sun, X., Zhu, L., Wang, F., Ma, Y., Niu, G., Hight Walker, A.R., Chen, X., 2013. ACS Nano 7(6), 5568-5576.
Liu, J., Jalali, M., Mahshid, S., Wachsmann-Hogiu, S., 2020. Analyst 145, 364-384.
Liu, X., Dai, Q., Austin, L., Coutts, J., Knowles, G., Zou, J., Chen, H., Huo, Q., 2008. J. Am. Chem. Soc. 130(9), 2780-2782.
Liu, X., Zhang, Y., Liang, A., Ding, H., Gai, H., 2019. Chem. Commun. 55(76), 11442-11445.
Loiseau, A., Asila, V., Boitel-Aullen, G., Lam, M., Salmain, M., Boujday, S., 2019a. Biosensors 9(2), 78-116.
Loiseau, A., Zhang, L., Hu, D., Salmain, M., Mazouzi, Y., Flack, R., Liedberg, B., Boujday, S., 2019b. ACS Appl. Mater. Interfaces 11(50), 46462-46471.
Lopez, A., Lovato, F., Hwan Oh, S., Lai, Y.H., Filbrun, S., Driskell, E.A., Driskell, J.D., 2016. Talanta 146, 388-393.
Lou, S., Ye, J.-y., Li, K.-q., Wu, A., 2012. Analyst 137(5), 1174-1181.
Makaraviciute, A., Ruzgas, T., Ramanavicius, A., Ramanaviciene, A., 2014. Anal. Methods. 6(7), 2134-2140.
Makaraviciute, A., Jackson, C.D., Millner, P.A., Ramanaviciene, A., 2016. J. Immunol. Methods 429, 50-56.
Malaspina, D.C., Longo, G., Szleifer, I., 2017. PLoS One 12(9), e0185518-e0185538.
Mie, G., 1908. Ann. Phys. 330(3), 377-445.
Moeremans, M., Daneels, G., Van Dijck, A., Langanger, G., De Mey, J., 1984. J. Immunol. Methods 74(2), 353-360.
Montenegro, J.-M., Grazu, V., Sukhanova, A., Agarwal, S., de la Fuente, J.M., Nabiev, I., Greiner, A., Parak, W.J., 2013. Adv. Drug Delivery Rev. 65(5), 677-688.
Mustafaoglu, N., Kiziltepe, T., Bilgicer, B., 2017. Nanoscale 9(25), 8684-8694.
Neves-Petersen, M.T., 2006. Protein Sci. 15(2), 343-351.
Niemeyer, C.M., Ceyhan, B., 2001. Angew. Chem. Int. Ed. 40(19), 3685-3688.
Nisnevitch, M., Firer, M.A., 2001. J. Biochem. Biophys. Methods 49(1), 467-480.
Peng, Z.G., Hidajat, K., Uddin, M.S., 2004. J. Colloid Interface Sci. 271(2), 277-283.
Pollitt, M.J., Buckton, G., Piper, R., Brocchini, S., 2015. RSC Adv. 5(31), 24521-24527.
Preechakasedkit, P., Osada, K., Katayama, Y., Ruecha, N., Suzuki, K., Chailapakul, O., Citterio, D., 2018. Analyst 143(2), 564-570.
Qian, X., Peng, X.H., Ansari, D.O., Yin-Goen, Q., Chen, G.Z., Shin, D.M., Yang, L., Young, A.N., Wang, M.D., Nie, S., 2008. Nature Biotechnol. 26(1), 83-90.
Raoof, M., Corr, S.J., Kaluarachchi, W.D., Massey, K.L., Briggs, K., Zhu, C., Cheney, M.A., Wilson, L.J., Curley, S.A., 2012. Nanomedicine 8(7), 1096-1105.
Rayavarapu, R.G., Petersen, W., Ungureanu, C., Post, J.N., van Leeuwen, T.G., Manohar, S., 2007. Int. J. Biomed. Imaging 2007, 1-10.
Rayner, S.L., Stephenson, F.A., 1997. Biochem. Soc. Trans. 25(3), 546S-546S.
Ruiz, G., Tripathi, K., Okyem, S., Driskell, J.D., 2019. Bioconjugate Chem. 30(4), 1182-1191.
Safenkova, I.V., Zherdev, A.V., Dzantiev, B.B., 2010. J. Immunol. Methods 357(1-2), 17-25.
Saha, B., Evers, T.H., Prins, M.W.J., 2014. Anal. Chem. 86(16), 8158-8166.
Saha, K., Agasti, S.S., Kim, C., Li, X., Rotello, V.M., 2012. Chem. Rev. 112(5), 2739-2779.
Schneider, G., Decher, G., Nerambourg, N., Praho, R., Werts, M.H.V., Blanchard-Desce, M., 2006. Nano Lett. 6(3), 530-536.

Sepulveda, B., Angelome, P.C., Lechuga, L.M., Liz-Marzan, L.M., 2009. Nano Today 4(3), 244-251.
Sharma, H., Mutharasan, R., 2013. Anal. Chem. 85(4), 2472-2477.
Sharma, P., Kumar, B., Suri, C.R., 2012. Environ. Pollut. 1(1), 12-19.
Špringer, T., Chadtová Song, X., Ermini, M.L., Lamačová, J., Homola, J., 2017. Anal. Bioanal. Chem. 409(16), 4087-4097.
Stringer, R.C., Schommer, S., Hoehn, D., Grant, S.A., 2008. Sens. Actuators B 134(2), 427-431.
Stuchinskaya, T., Moreno, M., Cook, M.J., Edwards, D.R., Russell, D.A., 2011. Photochem. Photobiol. Sci. 10(5), 822-831.
Tang, L., Li, J., 2017. ACS Sensors 2(7), 857-875.
Thébault, P., Boujday, S., Senechal, H., Pradier, C.-M., 2010. J. Phys. Chem. B 114(32), 10612-10619.
Tokuyasu, K.T., 1983. J. Histochem. Cytochem. 31(1A), 164-167.
Trilling, A.K., Beekwilder, J., Zuilhof, H., 2013. Analyst 138(6), 1619-1627.
Tripathi, K., Driskell, J.D., 2018. ACS Omega 3(7), 8253-8259.
Uludag, Y., Tothill, I.E., 2012. Anal. Chem. 84(14), 5898-5904.
Van Der Heide, S., Russell, D.A., 2016. J. Colloid Interface Sci. 471, 127-135.
Vdovenko, M., Byzova, N., Zherdev, A., Dzantiev, B., Sakharov, I.Y., 2016. RSC Adv. 6(54), 48827-48833.
Vikholm-Lundin, I., Albers, W.M., 2006. Biosens. Bioelectron. 21(7), 1141-1148.
Vörös, J., 2004. Biophys. J. 87(1), 553-561.
Wan, L., Zheng, R., Xiang, J., 2017. Vib. Spectrosc. 90, 56-62.
Wang, H., Wu, J., Li, J., Ding, Y., Shen, G., Yu, R., 2005. Biosens. Bioelectron. 20(11), 2210-2217.
Wang, J., Wang, L., Sun, Y., Zhu, X., Cao, Y., Wang, X., Zhang, H., Song, D., 2010. Colloids Surf. B 75(2), 520-525.
Wang, W., Wang, W., Liu, L., Xu, L., Kuang, H., Zhu, J., Xu, C., 2016. ACS Appl. Mater. Interfaces 8(24), 15591-15597.
Wang, X., Mei, Z., Wang, Y., Tang, L., 2017. Beilstein J. Nanotechnol. 8(1), 372-380.
Wang, Y., Tang, L.J., Jiang, J.H., 2013. Anal. Chem. 85(19), 9213-9220.
Welch, N.G., Scoble, J.A., Muir, B.W., Pigram, P.J., 2017. Biointerphases 12(2), 02D301.
Wu, X., Chen, X., Gao, F., Ma, W., Xu, L., Kuang, H., Li, A., Xu, C., 2016. Biosens. Bioelectron. 75, 55-58.
Xiao, M., Xie, K., Dong, X., Wang, L., Huang, C., Xu, F., Xiao, W., Jin, M., Huang, B., Tang, Y., 2019. Anal. Chim. Acta 1053, 139-147.
Xie, Y., Chang, H., Zhao, K., Li, J., Yang, H., Mei, L., Xu, S., Deng, A., 2015. Anal. Methods. 7(2), 513-520.
Yguerabide, J., Yguerabide, E.E., 1998. Anal. Biochem. 262(2), 157-176.
Yoshimoto, K., Nishio, M., Sugasawa, H., Nagasaki, Y., 2010. J. Am. Chem. Soc. 132(23), 7982-7989.
Zhang, L., Salmain, M., Liedberg, B., Boujday, S., 2019a. ACS Appl. Nano Mater. 2(7), 4150-4158.
Zhang, L., Hu, D., Salmain, M., Liedberg, B., Boujday, S., 2019b. Talanta 204, 875-881.
Zhao, H., Brown, P.H., Schuck, P., 2011. Biophys. J. 100(9), 2309-2317.

- The existing methodologies for antibodies attachment to gold nanoparticles through physical or chemical adsorption are described

- The challenging question of the quantification of antibodies on gold nanoparticles surface is critically addressed

- The importance of mastering the association antibody/gold nanoparticles is highlighted

- A selection of relevant application of gold nanoparticles antibody bioconjugates in optical biosensing is presented

Declaration of interests

☒ The authors declare that they have no known competing financial interests or personal relationships that could have appeared to influence the work reported in this paper.

☐The authors declare the following financial interests/personal relationships which may be considered as potential competing interests: